UNIVERSITY OF CALIFORNIA,
IRVINE

Experimental Evaluation of Two-Way Sandwich Paneled Slabs

THESIS

submitted in partial satisfaction of the requirements
for the degree of

MASTER OF SCIENCE

In Civil Engineering

by

Surbhi Dadlani

Thesis Committee:
Professor Ayman S. Mosallam
Associate Professor Farzin Zareian
Assistant Professor Anne Lemnitzer

2015

DEDICATION

I dedicate this thesis to my Professor Dr. Ayman S. Mosallam for without his support, encouragement and coaching this would have never been possible.

TABLE OF CONTENTS

LIST OF FIGURES

LIST OF TABLES

ACKNOWLEDGMENT

Firstly, I would like to express my sincere gratitude to my advisor Professor Dr. Ayman S. Mosallam, for his continuous support, patience, motivation, and contribution of immense knowledge throughout my Master's Program and related research. His guidance helped me throughout the time of research and writing of this thesis. I could not have imagined having a better advisor and mentor for my study.

Besides my advisor, I would like to thank the rest of my thesis committee, Professor Farzin Zareian and Professor Anne Lemnitzer, for their insightful comments and encouragement, which incented me to widen my research from various perspectives.

I thank my fellow the members of my research group Islam Rabie, Jivan Pachpande, Rahil Shrivastava, Ehsan Mimateghi for the stimulating discussions, support and great efforts to accomplish this research.

Last but not the least; I would like to thank my family for their constant moral support and encouragement for the successful completion of my thesis.

ABSTRACT OF THE THESIS

Experimental Evaluation of Two-Way Sandwich Paneled Slabs

By

Surbhi Dadlani

Master of Science in Civil Engineering

University of California, Irvine, 2015

Professor Dr. Ayman S. Mosallam, Chair

This research focuses on the experimental evaluation of the flexural behavior of light-weight two-way slabs made of three-dimensional (3D) sandwich panels subjected to out-of-plane loading. The sandwich panels evaluated in this study were composed of two exterior faces made of high-strength mortar reinforced with bidirectional cold-rolled steel wires. The sandwiched core consists of fire retardant Expanded PolyStyrene (EPS) foam core. In this study, three square large-scale sandwich slab specimens with different dimensions and spans were subjected to mid-span loads up to failure. All specimens were instrumented with electrical strain gages and string potentiometers to monitor steel and mortar strain variations and deflections. During each experiment, loads, strains, and vertical deflections were monitored and the results were analyzed. Load-deflection (P/δ) and stress-strain (σ/ε) curves were also developed for each specimen at different locations. Cracks initiation and propagation were monitored throughout each test and crack mapping was performed for each slab specimen. Peak load, ultimate strain, and maximum vertical

displacement were observed and the failure load for each specimen was identified and recorded. A simplified analytical procedure that followed the requirements of ACI 318-14 was developed to provide conservative estimates of the capacity of each structural sandwich slab evaluated in this study. Experimental results were compared with the predicted capacity and deflection of each sandwich slab specimen and a good agreement was achieved in the linear range.

CHAPTER 1

INTRODUCTION

Sandwich panels are being extensively and increasingly used in single-story and multistory building construction because of their unique attractive features such as light-weight that eliminates the need of heavy transportation and installation equipment. Such features help in achieving rapid construction, superior thermal and acoustic insulation properties. Sandwich panels have been used as structural building components in residential, industrial and commercial buildings in many countries.

1.1. Composite Floor Panels with EPS Foam Core

The sandwich panels used in this study were manufactured by Schnell™ Home S.R.L., Italy. These sandwich panels consist of two exterior high-strength steel wire mesh and cementitious mortar facings connected via shear wire connectors with fire retardant expanded polystyrene (EPS) foam core (see Figure (1.1)). These sandwich panels have superior flexural stiffness due to optimized allocation of materials in accordance to the flexural demand. As illustrated in Figure (1.1), the strain distribution for a structural element subjected to flexure has maximum value at the extreme fibers that diminishes as it approaches the neutral axis location. Thus, placing stronger materials at the exterior faces with relatively less stiff material around the neutral axis will produce an optimum flexure capacity. This concept has

been adopted by the aerospace industry for many decades due to the priority of decreasing the dead weight of air vehicles and structures. In our case, the same concept is applied by placing cementitious bi-directionally reinforced high-strength mortar shells at the extreme fibers of the panels while the inner portion is filled with a relatively cheaper and weak material such as EPS foam. This will result in an appreciable amount of decrease in cementitious materials, leading to a more environmental friendly and energy efficient building material (as a rule of thumb, one ton of cement produces about one ton of carbon dioxide emission [Malhotra, 1998]). The reinforced concrete faces take compressive and tensile loads resulting in higher stiffness and strength and the core transfers the shear loads between the faces. The choice of selecting the EPS foam as filling core is an excellent approach due to its extremely light-weight property, in addition to its superior thermal and acoustic insulation properties. Besides these advantages, the expanded polystyrene foam core also has construction viability by providing support mechanism for the two steel wire meshes during construction. Hence, expanded polystyrene sandwich panels represent an excellent example of the optimum use of dissimilar materials.

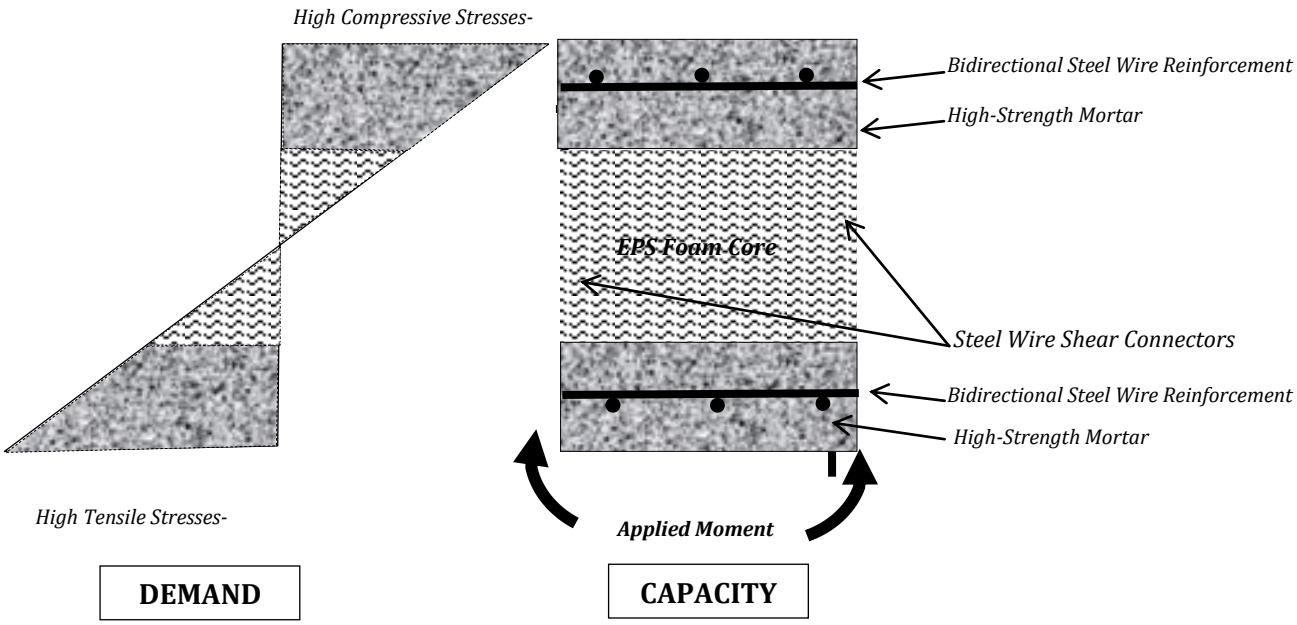

Figure (1.1): Optimum Materials Allocation of a Typical Sandwich Panel Construction

The following are some of the benefits of the light-weight sandwich panels:

- Easy installation due to its light-weight.
- Reduces carbon emission due to minimum use of cement.
- Elimination of the need of heavy transportation and site construction equipment.
- Ability to use recycled steel and foam materials.
- Superior thermal and acoustic insulation.
- Superior impact and fire resistance.
- Materials and construction costs are less, thus making it apt for affordable housing applications.

1.2 .Research Significance and Objective

Most of the sandwich panel construction is confined to panelized construction. Panelized construction is a method where the building is subdivided into basic planar elements that are typically constructed under some form of mass production. They are then shipped directly to the construction site and assembled into the finished structure. This research is concerned with sandwich panels having concrete-steel faces and polystyrene core materials which can be casted on site and will be cheaper as well.

As the use of expanded polystyrene foam in the middle of concrete-steel facings is a relatively new concept, there is a need to verify the applicability of such new panels in order to develop the necessary confidence among manufacturers and designers. This clearly indicates the need for research to investigate the behavior of concrete expanded polystyrene (CEPS) sandwich panels. Hence, this research works towards achieving accurate design recommendations for concrete expanded polystyrene (CEPS) sandwich panels among manufacturers and designers. This research on the structural evaluation of sandwich panels is intended to utilize the sandwich panels in a manner that is safe and reliable. There are different kinds of sandwich panels that have been used. However, research is needed to investigate issues associated with the development of sandwich panels as a slab flooring system. Therefore, the scope of this research focuses on the structural evaluation of sandwich panels as slab flooring systems.

1.3. Overall Objective

The main purpose of this research is to conduct a thorough investigation of the behavior of CEPS sandwich panels and predict load deformation curves.

1.4. Method of Investigation

This dissertation is based on a series of laboratory experiments performed at the University of California, Irvine (UCI). Laboratory experiments include the concentrated loading test performed on three different CEPS sandwich panels. Experimental results were recorded and compared with predicted results.

1.5. Dissertation Overview

This dissertation consists of five chapters. Chapter 1 presents an introduction to the principal reasons for the commencement of this research, followed by the research significance and objectives of this dissertation. Chapter 2 provides an overview of the work related to this research including past research on sandwich panels, material properties, and relevant standards.

The chapters, Chapter 3 through Chapter 5, include the main body of the dissertation. Chapter 3 has a description about the test specimens and discussions about the experimental results. Chapter 4 describes analytical results as per ACI 318-14 code and Chapter 5 discusses the conclusions and recommendations for future research on two way sandwich paneled systems.

CHAPTER 2

LITERATURE REVIEW

2.1. Introduction

New materials and new combinations of old materials are constantly being proposed and used in sandwich panels. Sandwich panels have many engineering applications as they can be used as either wall, slab or beam. Karam and Gibson (1994) evaluated the wood-cement and natural fiber-cement to be used as a sandwich-panel facing by performing three-point bending test. Pokharel (2003) studied the behavior and design of sandwich panels made up of steel mesh on both faces and polystyrene foam as a core. The author further mentioned that the structural sandwich panels, generally used in Australia, comprise of polystyrene foam core and high strength (minimum yield stress of 550.0MPa and reduced ductility) steel faces bound together using separate adhesives.

Schenker et al. (2005) studied the behavior of reinforced concrete structures with aluminum foam under impact loading**.** Vaidya et al. (2010) demonstrated the panels which comprised of face sheets made up of E-glass fibers impregnated with polypropylene matrix and the core that was made up of expanded polystyrene foam. These panels were developed as exterior walls of a modularized structure. Manalo (2011) investigated the concept of glue-laminated composite sandwich beams which were made up of glass fiber composite skins and modified phenolic core material for railway turnout sleepers.

This research focuses on the use of EPS as a foam and concrete wire meshing as a face sheet which will be easier as well as less expensive to cast on site.

2.2. Concept and Function of Sandwich Panel

The concept behind sandwiched construction is to have the facings and core to act in unison as a very efficient structural element. The function of sandwich structures can be compared to that of I-sections, in which the facings of a sandwich panel (see Figure (2.1)) can be compared to the flanges of an I-beam, as they carry the bending stresses. The core corresponds to the web of the I-beam, as it resists the shear loads and stabilizes the faces against buckling or wrinkling (Zenkert 1995).

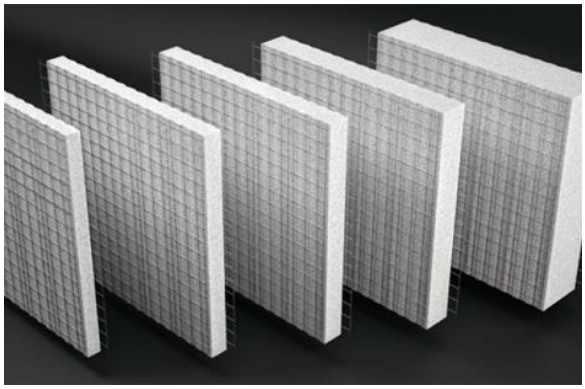

Figure (2.1): Typical Sandwich Panel

The core must be stiff enough to ensure that the facings remain separated by a proper distance. The core must also provide adequate shearing strength so that the facings will not slide relative to each other when the sandwich panel is bent. In the

absence of necessary shear strength, the two thin facings would act as two independent beams or panels, and lose the sandwich effect. Finally, the core must also possess enough stiffness so that the facings stay flat or nearly flat when they are subjected to compressive stresses that would otherwise cause buckling or wrinkling. The objective of the sandwich composite panels is to offer a structure that is strong and stiff but yet lightweight.

The major advantages of sandwich composites over conventional materials are due to the following properties of sandwich composites:

(1) Low overall density, high strength-to-weight ratio, and high stiffness-to weight ratio.

(2) Are capable of providing good thermal and acoustical insulation.

(3) Have uniform energy absorption capacity.

Such overall versatility has contributed greatly to the development of light-weight sandwich composites (Ueng 2001).

2.3. Material Properties of Sandwich Panels

CEPS panels are made up of three materials: concrete, steel and expanded polystyrene foam. Each of these materials have different characteristics. Concrete and mortar are heterogeneous materials made up of cement, water and aggregates. Mature, hardened concrete and high strength mortar have good compressive strength, typically between 30.0MPa (4351 psi) and 60 MPa (8702). Its mechanical properties scatter more widely and cannot be defined easily. For the convenience of

analysis and design, however, concrete is often considered a homogeneous material in the macroscopic sense. Steel can be considered a homogeneous material and its material properties are generally well defined. On the other hand, EPS is a light-weight material with good insulation and energy absorption characteristics (Mousa and Uddin 2010).The resulting combination of these materials will be good for efficient load resistance as well as thermal insulation. The properties of these materials are discussed in detail.

2.3.1. **Stress-Strain Curve of Concrete**

There are several models reported in the literature to illustrate the stress-strain behavior of concrete. Among them, one proposed by Bangash (2001) is shown in the Figure (2.2). According to Bangash (2001), experimental tests show that concrete behaves in a highly nonlinear manner in uniaxial compression. The stress-strain curve of concrete is linearly elastic up to 30% of the maximum compressive strength. Above this point the curve increases gradually up to about 70-90% of the compressive strength. Eventually, it reaches the peak value, and then stress-strain curve descends. After the curve descends, crushing failure occurs at an ultimate strain ε_{cu}.

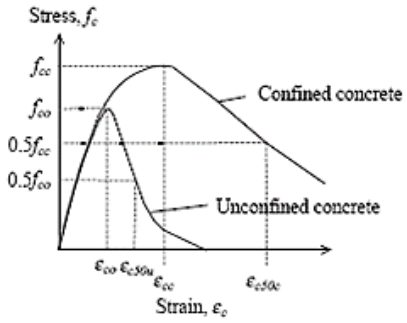

Figure (2.2): Typical Stress-Strain Curve of Confined and Unconfined Concrete

Several researchers have estimated the values for the stress strain curve of concrete. Collins and Mitchell (1994) suggested the stress-strain relation of concrete in compression as shown in Table (2.1). Rots et al. (1985) suggested the stress- strain relation of concrete in tension as shown in Table (2.2).

Table (2.1): Values of the Stress-Strain Curve for Mortar

Parameter	**Compression**
Peak stress	$f_c^{'}$
Peak strain	$\varepsilon_{co} = 0.00 + \frac{fc'}{70000}$
Ultimate stress	f_{c1} = 12 MPa
Ultimate strain	ε_{c1} = 0.0036
Failure strain	ε_{SD}= 0.012 – 0.0001 $f_c^{'}$

Table (2.2) Values of the Stress-Strain Curve for Concrete in Tension
[Source: Rotset al., 1985]

Parameter	Tension
Peak Stress	$f_t' = 0.625\sqrt{f_c'}$
Peak Strain	$\varepsilon_{ct} = 0.10\varepsilon_{co}$
Ultimate Stress	$f_t^1 = \frac{f_t'}{3}$
Ultimate Strain	$\varepsilon_{t1} = \frac{2\varepsilon_u}{9}$

2.3.2. Expanded Polystyrene Foam (EPS)

The Expanded Polystyrene (EPS) foam is a lightweight, closed-cell, hydrophobic (moisture repellent), thermoplastic material. The EPS foam used in this study has low thermal conductivity, high acoustic resistance coupled with high shock absorption. It is also a recyclable material that can be reused in different applications such as lightweight concrete, building products and can be remolded back to produce EPS foam cores of the sandwich panels.

Structural properties of EPS

Figure (2.3) shows a typical stress-strain curve of EPS foam under monotonic compression loads. As shown in this figure, the behavior is generally linear up to

about 1 to 2% compression strain. It should be noted that the elastic limit of EPS foam is a function of its density. So, as the density increases, this linear limit increases. The stress-strain behavior is also an inverse function of temperature; for example, as the temperature decreases, the compressive strength of the EPS increases. The compressive stress is measured by identifying a single-value at some arbitrary strain level. This arbitrary strain level is commonly taken as 10% which approximately corresponds to the end of the yield range. The value of the slope of this initial portion is known as initial tangent modulus or Young's Modulus of elasticity. For low compressive strains up to approximately 1%, EPS appears to behave linearly and an initial tangent Young's modulus of elasticity, E_{ti}, can be defined, which exhibits an approximately linear correlation with the EPS density. Eriksson and Tränk (1991) obtained the following empirical relationship for the E_{ti} as a function of foam density:

$$E_{ti} = 0.0097\,\rho^2 - 0\text{-}014\rho + 1.80 \quad (2.1)$$

where ρ is the EPS density, ρ (kg/m^3).

A simpler relation for obtaining E_{ti} was proposed by Magnan and Serratrice (1989):

$$E_{ti} = 0.0479\,\rho - 2.875 \quad (2.2)$$

Several researchers have estimated values of Poisson's ratio (ν) for EPS foam materials. Eriksson and Tränk (1991) estimated the Poisson's ratio to be taken approximately 0.05 under initial loading. In 1995, Horvath reported that within the initial linear range of the compressive stress-strain curve, the ν value can be

estimated from the following empirical relationship:

$$\nu = 0.0056\rho + 0.0024 \quad (2.3)$$

However, the Poison's ratio could be a negative value or close to zero as suggested by Negussey and Jahanandish (1993).

Since EPS foam is a viscoelastic material, it is essential that the time-dependent creep deformation be taken into account. The time-dependent behavior includes both creep (time-dependent deformation under sustained load), and relaxation(time-dependent stress change when EPS foam is subjected to sustained deformation under constant deformation). Figure (2.3) presents stress-strain curves for EPS with density of 23.5 kg/m^3 for different durations of loading up to 10,000 hours (Horvath, 1994).

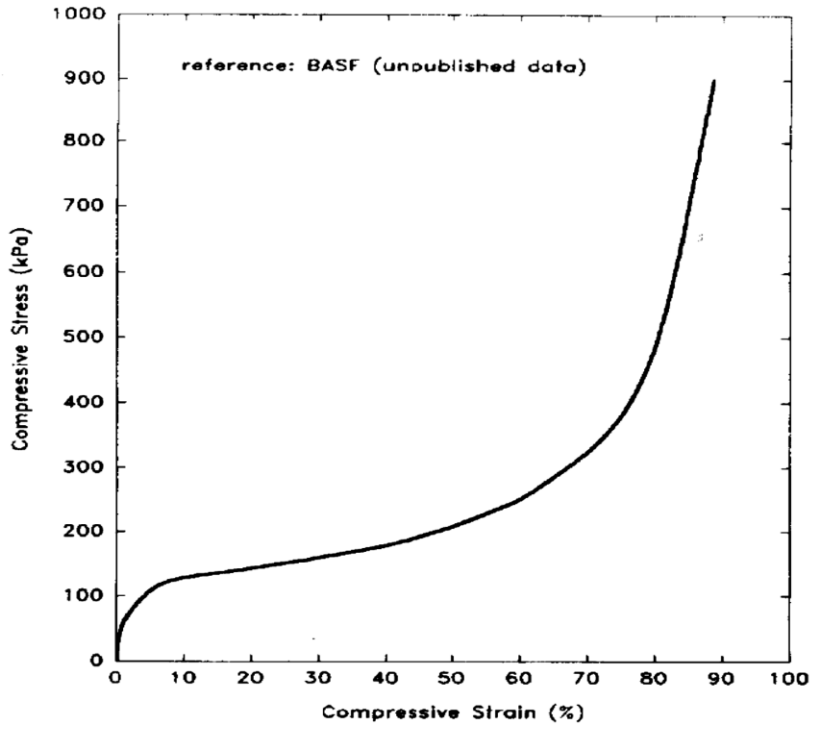

Figure (2.3): Load-Deformation Behavior of 21 kg/m3 EPS under Short-Term Unconfined Axial Compression Loading. [Horvath, 1994]

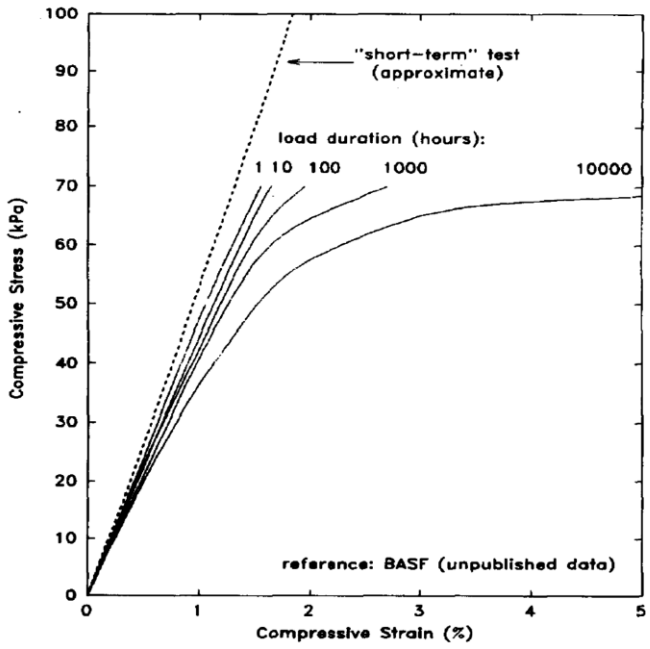

Figure (2.4): Time-Dependent Stress Strain Behavior of 23.5 kg/m^3 EPS in Unconfined Axial Compression [Horvath, 1994]

CHAPTER 3

DESCRIPTION OF THE EXPERIMENTAL PROGRAM

3.0 General

In this chapter, a detailed description of the experimental program is presented. This includes information on test specimens dimension and geometry, different material properties used in fabricating the sandwich slab specimens, boundary support design and construction, instrumentation techniques and specifications of sensors used. In addition, description of loading protocol and test setup are also discussed. Experimental load-deflection and load-strain cures are presented and discussed.

3.1 Description of Slab Specimens

The sandwich panels evaluated in this study consists of a three-dimensional (3D) welded-wire space truss incorporating through-the-thickness wires welded to welded-wire reinforcement (WWR) on each side of an integral core. The core is made of fire-retardant Expanded PolyStyrene(EPS) foam (see Figure (3.1)).

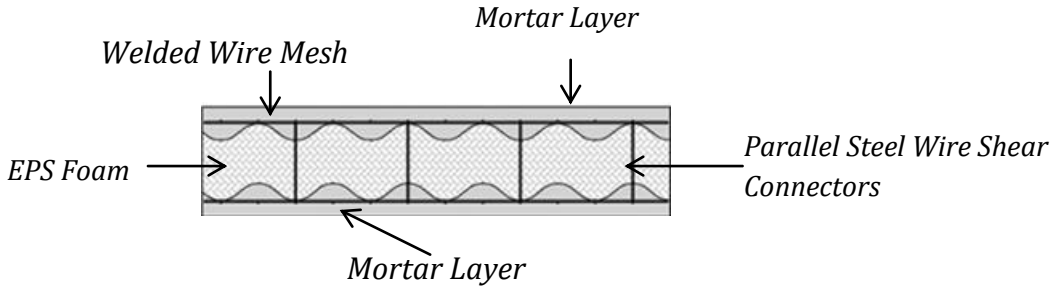

Figure (3.1): Typical Section of Sandwich Panels with Parallel Wire Shear Connectors

In order to fabricate these panels as structural members, the sandwich panels must be placed in position, and a Wythe of high-strength mortar or concrete is applied to each side of the faces of the EPS foam core covering the bidirectional welded wire reinforcement (WWF).The steel wire mesh layout was same for the three slab specimens. The different dimensions of the three sandwich slab specimens evaluated experimentally in this investigation are summarized in Table (3.1) and Figures(3.2), and (3.3).

Table (3.1): Description of Sandwich Slab Specimens

Test Specimen ID	Length x Width	Thickness
A	3.0m x 3.0m (132.0 in x 132.0in)	0.30 m (12.0 in)
B	3.0m x 3.0m (132.0 in x 132.0in)	0.27 m (10.5 in)
C	4.0m x 4.0m (172.0 in x 172.0in)	0.30 m (12.0 in)

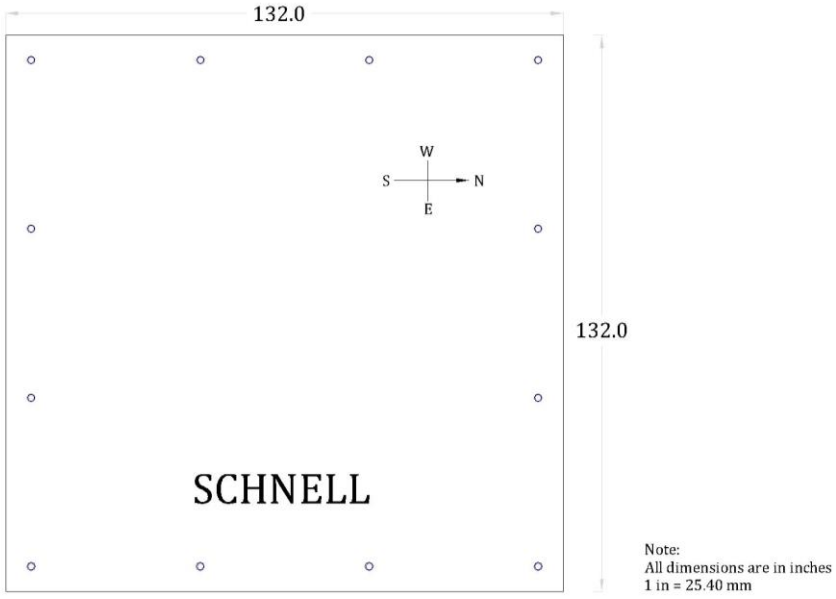

Figure (3.2): Layout of Sandwich Slab Specimens A and B

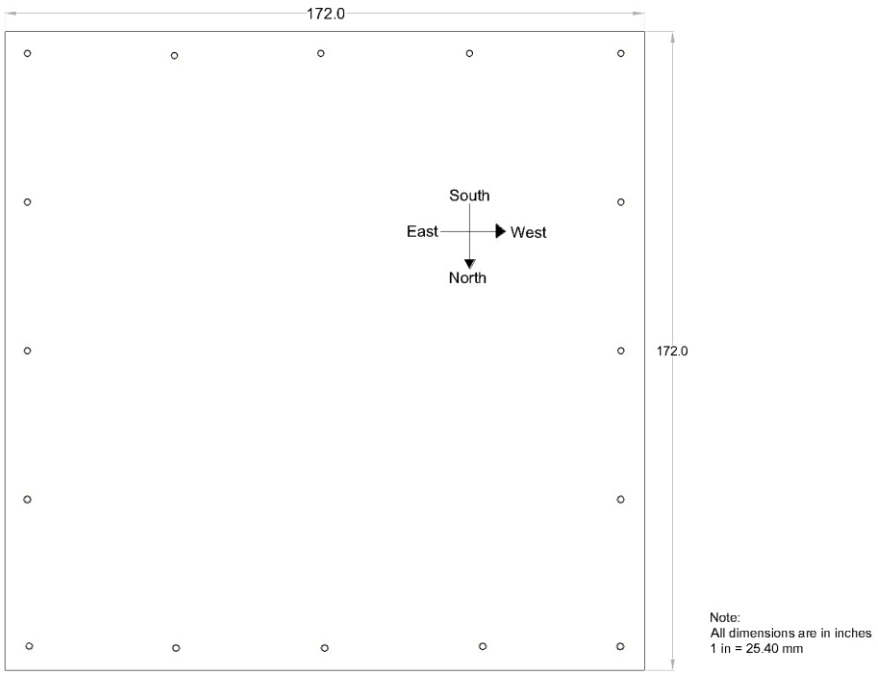

Figure (3.3): Layout of Sandwich Slab Specimen C

3.1.1. Materials

As stated earlier, the materials used in the construction of the sandwich test slabs consisted of cold-rolled steel wire mesh, expanded polystyrene foam core, and through-the-thickness parallel steel shear connectors and high-strength mortar. Description of the materials is discussed in the following sections.

3.1.2. Expanded Polystyrene (EPS) Foam Plastic Core

The core is Type I modified EPS foam plastic complying with ASTM C578, having a normal density of 1.0 pound per cubic foot (16.0kg/m^3) as manufactured by Poliestireno Alfa Gamma, S.A. de C.V., Insulfoam, LLC and Fanosa S.A. de C.V. The insulation has a flame-spread index of 25 or less and a smoke-developed index of

450 or less when tested in accordance with ASTM E84 at a 6-inch (152.0mm) thickness for EPS boards recognized under ICC-ES ESR-1788 and ESR-1006, and at a 4.0inch (102mm) thickness for EPS boards recognized under ICC-ES ESR-2744.

3.1.3. Reinforcement

The floor panels consist of a welded wire space frame integrated with fire retardant EPS foam core. The panel receives its strength and rigidity by the diagonal 9-gauge cross wires welded to the3.15in X 2.95in (80mm X 75mm) cold-rolled steel wire fabric on each side. This produces a truss behavior which provides rigidity and shear transfer for full composite behavior. The diagonal nine gauge cross wires are pushed through the poly core and welded with automated equipment. The 9-gauge (3.0mm) galvanized cold-rolled welded wire fabric conforms to A.S.T.M A-185 and A.S.T.MA-82. Figure (3.4) shows the sandwich panel specimens.

Figure (3.4): Test Specimens prior to Mortar Application

3.1.4. High-Strength Mortar

The cementitious mortar used in fabricating the sandwich slab specimens was ready-mixed. The high-strength mortar was ordered to meet the following specifications:

1. Minimum of 2,500 psi (17.2 MPa) 28-day compressive strength.
2. 3/8 inch (9.5 mm) maximum size crushed aggregate.
3. Minimum slump of 2.0 inches (51.0 mm).
4. No reducing agents or admixtures.

The 28-day mortar compressive strength, f'_c was determined from an average of 8.0" x12.0"(203 mm X 305 mm) control cylinders tested in accordance with ASTM C39-71. Testing of the cylinders occurred within one day of testing of slab specimens. Modulus of rupture and split cylinder strengths were determined by ASTM C78-64 and ASTM C496-71 standards, respectively. The 28-day mortar compressive strength for the tested cylinders is presented in Tables(3.2), (3.3) and (3.4).

Table (3.2): 28-Day Mortar Compressive Strength for Sandwich Slab Specimen "A"

Compression Specimens	**Compression Force kN(lb)**	**Compressive Strength kN/mm² (psi)**	**Average Compressive Strength kN/mm² (psi)**
Cylinder Dimensions: 4" (102 mm) Diameter 8" (203 mm) Height	282.0(63,435.0)	33,929.0(4,921.0)	33,370.0 (4,840.0)
	279.0(62,670.0)	33,943.0(4,923.0)	
	265.0(59,525.0)	32,240.0(4,676.0)	

Table (3.3): 28-Day Mortar Compressive Strength for Sandwich Slab Specimen "B"

Compression Specimens	**Compression Force kN(lb.)**	**Compressive Strength kN/mm² (psi)**	**Average Compressive Strength kN/mm² (psi)**
Cylinder Dimensions: 4" (102 mm) Diameter 8" (203 mm) Height	276.0(62,000.0)	33,577.0(4,870.0)	32,950.0 (4,779.0)
	273.0(61,500.0)	33,308.0(4,831.0)	
	262.0(59,000.0)	31,957.0(4,635.0)	

Table (3.4): 28-Day Mortar Compressive Strength for Sandwich Slab Specimen "C"

Compression Specimens	**Compression Force kN(lb)**	**Compressive Strength kN/mm² (psi)**	**Average Compressive Strength kN/mm² (psi)**
Cylinder Dimensions: 4" (102 mm) Diameter 8" (203 mm) Height	286.0(64,340.0)	35,321.0(5123)	33,748.0 (4,895.0)
	274.0(61,670.0)	33,853.0(4910.0)	
	260.0(58,430.0)	32,074.0(4652.0)	

3.2. Fabrication, Casting, and Curing of Sandwich Slabs

3.2.1. Fabrication: All the Schnell Home S.R.L. Expanded Polystyrene (EPS) Sandwich Panels used for fabricating the floor specimens were randomly sampled by the P.I. (Dr. Ayman Mosallam representing UCI IAS accredited facility TR318) at the Schnell Home S.R.L. warehouse in Fano, Italy. It was ensured that the panels fulfill the requirements of the ICC-ES AC 85 section 3.1 and are truly representative of the standard Schnell Home S.R.L. manufactured product for which recognition is being sought. The inspection and selection process was performed on October 15, 2012 at the manufacturer facility in Italy. All the randomly selected panels were inspected for overall dimensions, mil certificates, steel wire diameters for both face grids and through-the-thickness connectors, the total thickness of each panel, and the spacing of all face grids. Each panel was inspected, labeled and signed by the inspector and all labeled panels were ready for direct shipping to UCI testing facility in Irvine, California, USA. Upon receiving the panels at UCI facility, all the signed labels

were checked and were confirmed. Figures (3.5), (3.6), (3.7) and (3.8) show samples of photographs illustrating inspection procedures. In addition, process of fabricating the samples at UCI facility that included applying the cementitious face layers were monitored, and inspected by UCI lab staff in accordance to the standard procedure used in the site for this product.

Figure (3.5): Measurement of Welded Wire Mesh

Figure (3.6): Measurement of Diameters of WWF Wires

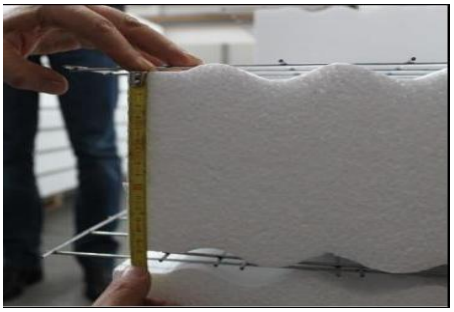

Figure (3.7): Measurement of Thickness of EPS between WWF

Figure (3.8): Labeling of panels

3.2.2. Casting of Face Sheet High-Strength Mortar

Placing of high-strength mortar for the three sandwich slabs was performed on 10/28/2014. The high-strength mortar was delivered by a conventional ready-mix

truck and was poured on the slabs with help of a pump. Upon delivery, slump tests meeting ASTM C143-71 specifications were taken to determine the amount of water needed to bring the slump within the specified range. Periodically, during casting, additional slump tests were taken as a check on the consistency of concrete placement. However, the slump reading for Batch ID III was 8.0"(203.30mm)as it was taken in the end. Figure (3.9) shows measurement of the slump being done in laboratory.

Figure (3.9): Measurement of Slump at UCI SETH Laboratory

Table (3.5): Mortar Slump Measurements

Batch ID	**Slump Value, mm (in)**	**Temperature °C (°F)**	**Relative Humidity** (%)
I	127.0 (5.0)	25.0 (77.0)	66
II	51.0 (2.0)	26.0 (79.0)	65
III	203.3 (8.0)	26.0 (79.0)	63

Verification mortar cylinder specimens were prepared in accordance with ASTM C31 specifications. The cylinders were made using 8"x12"(203 mm X 305 mm)

plastic cylinder molds and cast at intervals during the concrete pouring of the slabs so as to obtain the average concrete strength(see Tables (3.2), (3.3) and (3.4)).

Placing of the high-strength mortar in the slabs began at the south end and progressed across the slab to the north end. Figure(3.10) and (3.11)shows the casted slab specimens

Figure (3.10): Pouring of High-Strength Mortar at UCI SETH Laboratory

Figure (3.11): Sandwich Slab Specimen after Placing the High-Strength Mortar

An internal vibrator supplied by the contractor was used to obtain satisfactory compaction and placement of the concrete. In the end, the contractor proceeded to trowel the final finish surface on the slabs. The surface was finished to a smooth texture to aid in placing strain gages on the concrete surface. During final finishing the lifting anchors were located and the concrete was sufficiently removed over them to allow insertion of the screw lift hooks.

3.2.3. Curing

Twenty-four hours later after the concrete was placed, all the slabs and cylinders were covered with plastic sheets. After seven days of curing, the plastic sheets were removed and all slabs were exposed to normal room conditions until tested. Throughout the curing from the time the slabs were cast until the time of testing, the laboratory temperature and humidity were continuously recorded on a hygro-thermograph.

3.3. Equipment Instrumentation.

Details of instrumentation and sensors used for recording the experimental measurements of the two-way sandwich slab specimens are described in the following sections.

3.3.1. Electronic Strain Gauges

Electronic strain gauges were attached on the top surface of the steel mesh and on the top surface of concrete. The labeling used for strain gauges and their location is summarized in Table (3.12) and Figures (3.12), (3.13), (3.14), (3.15), (3.16) and (3.17).

Table (3.6): Meaning of Symbols Used for Naming Concrete Strain Gauges

Symbol	Meaning
C	Mortar
S	Surface
A/B/C	Slab Specimen
U	Upper Surface

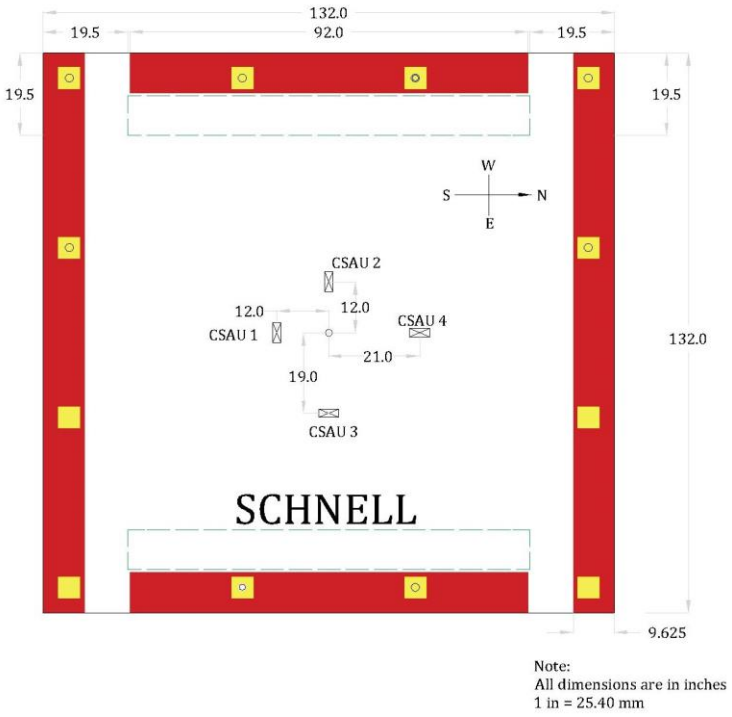

Figure (3.12): Concrete Strain Gauge Location for Slab Specimen A

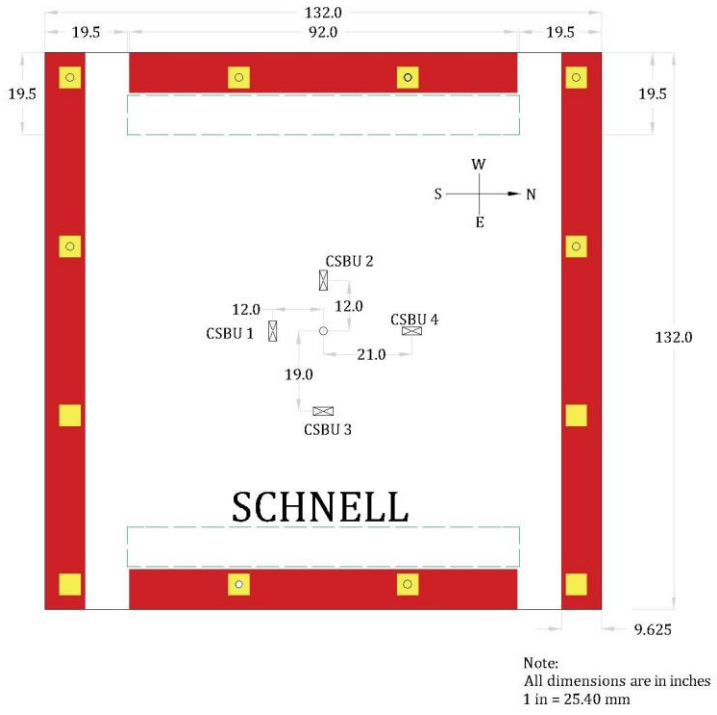

Figure (3.13): Concrete Strain Gauge Location for Slab Specimen B

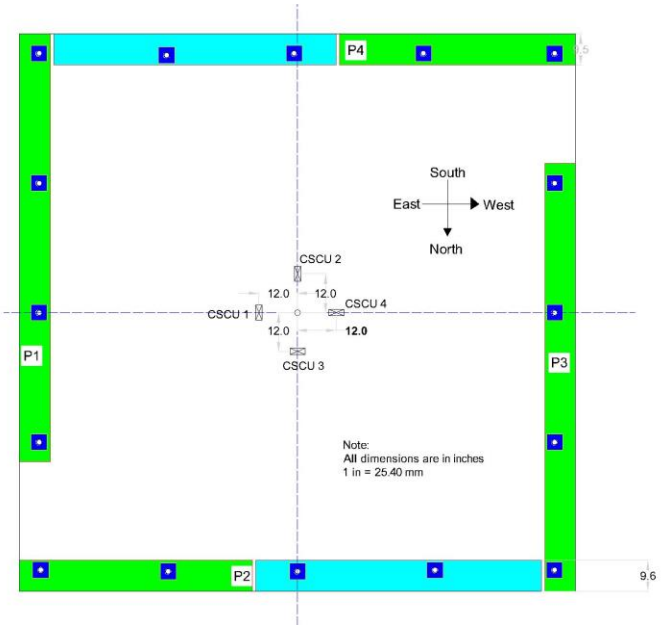

Figure (3.14): Concrete Strain Gauge Location for Slab Specimen C

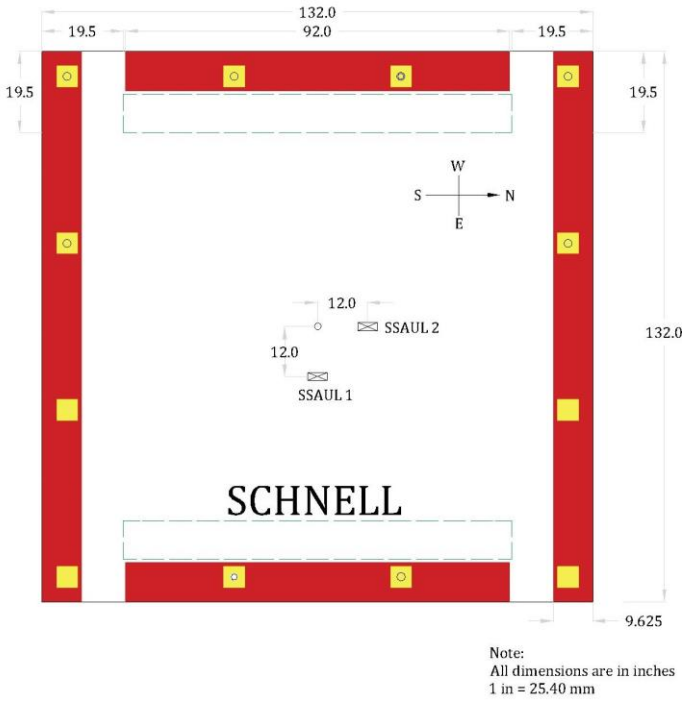

Figure (3.15): Steel Strain Gauge Location for Slab Specimen A

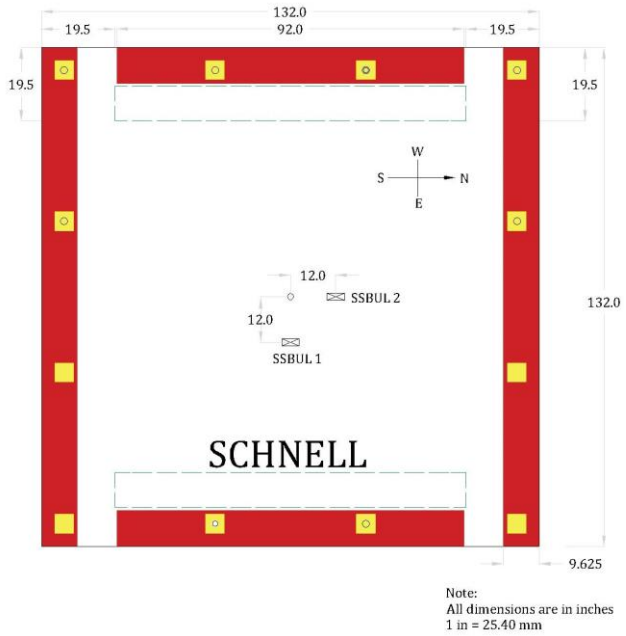

Figure (3.16): Steel Strain Gauge Location for Slab Specimen B

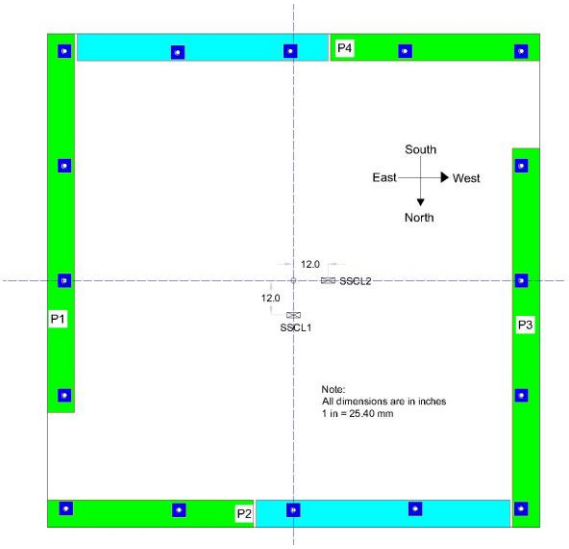

Figure (3.17): Steel Strain Gauge Location for Slab Specimen C

The specifications of the strain gauges used for steel and concrete surfaces are given in Table (3.6).

Table (3.7): Properties of Strain Gauges Bonded to Steel and Mortar Surfaces.

Property	Steel Surface Strain Gauges	Concrete Surface Strain Gauges
Gage Factor (24^{o}C, 50% RH)	2.09+- 1.0%	2.13 +- 0.35%
Gage Length	2.0 mm	2.0 mm
Gage Resistance	120.40 ± 0.40 Ω	120.0 ± 0.4 Ω
Adoptable Thermal Expansion	11.70 PPM per ^{O}C	11.7 PPM per ^{O}C
Temperature Coefficient of Gage Factor	0.008 % per ^{O}C	0.008 % per ^{O}C
Applicable Gage Cement	CC-33A, EP-34B	CC-33A, EP-34B

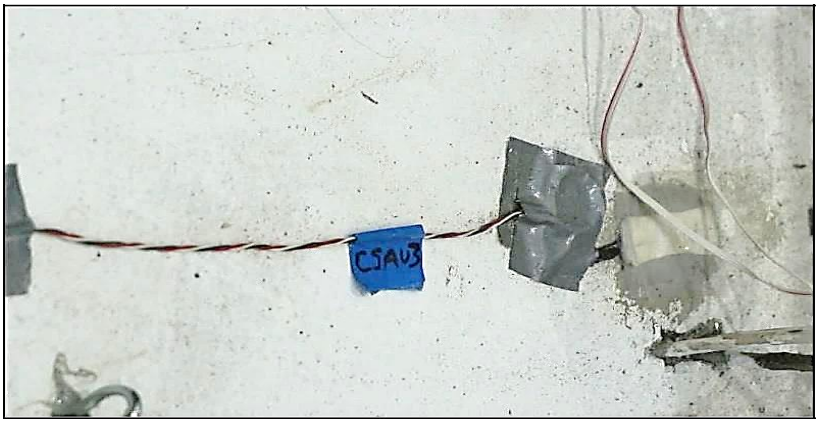

Figure (3.18): Strain Gauge on Mortar Surface.

3.3.2. Hydraulic Jack

A full monotonic load was applied via four ENERPAC® RCH-603 hollow plunger cylinders with a maximum operating pressure of 10,000 psi (68948 kN/mm^{2})and a

maximum stroke of 2.60”(66 mm). A pressure transmitter (Model WIKA Model S-10) was used to convert the pressure into an analog electrical signal for recording purposes. Figure (3.19) shows the Hydraulic jack assembly used for applying concentrated loading.

Figure (3.19): Hydraulic Jack Assembly.

3.3.3. Electronic String Potentiometers (String Pots)

String potentiometers were attached to the top concrete surface to determine the deflection of slab at locations determined by yield line theory. The description of the assembly used for attaching string potentiometers is discussed later in this chapter.

3.3.4. Data Acquisition System

A computerized Data Acquisition (DAQ) is the process of measuring an electrical or physical phenomenon such as voltage, current, temperature, pressure, or sound with a computer. A DAQ system consists of sensors, DAQ measurement hardware, and a computer with programmable software. Compared to traditional measurement systems, PC-based DAQ systems exploit the processing power, productivity, display, and connectivity capabilities of industry standard computers

providing a more powerful, flexible, and cost-effective measurement solution. Parts of a Data Acquisition system are described below:

a) **Sensors:** The measurement of a physical phenomenon, such as the temperature of a room, the intensity of a light source, or the force applied to an object, begins with a sensor. A sensor, also called a transducer, converts a physical phenomenon into a measurable electrical signal. Depending on the type of sensor, its electrical output can be a voltage, current, resistance, or another electrical attribute that varies over time. In this case the electrical output was voltage.

b) **DAQ Boards and Devices:** DAQ hardware acts as the interface between a computer and signals from the outside world. It primarily functions as a device that digitizes incoming analog signals so that a computer can interpret them. The three key components of a DAQ device used for measuring a signal are the signal conditioning circuitry, analog-to-digital converter (ADC), and computer bus. Many DAQ devices include other functions for automating measurement systems and processes. For example, digital-to-analog converters (DACs) analog signals, digital I/O lines input and output digital signals, and counter/timers count and generate digital pulses. Figures (3.20) and (3.21) show the Data Acquisition system used and the connections of strain gauges and string potentiometers to the Data Acquisition system.

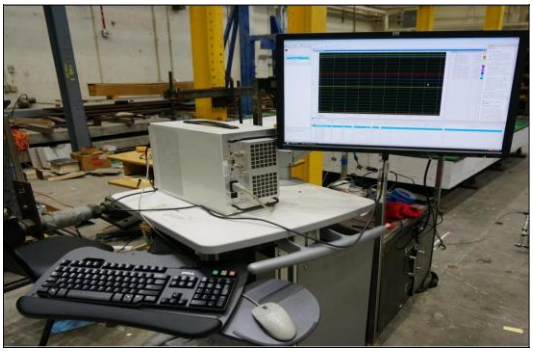

Figure (3.20): Data Acquisition System to Record Experimental Data

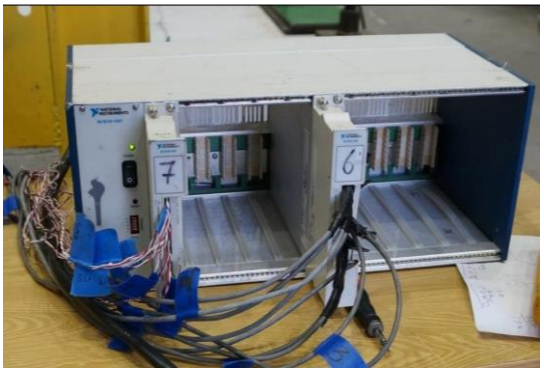

Figure (3.21): National Instrument Channel ADC

3.4 End Supports for Sandwich Slab Specimens

A steel test frame that consisted of various structural elements was used in all three full-scale sandwich slab specimen tests. The sandwich slab slabs were casted on a plywood frame placed on the floor of the laboratory. Figures (3.22) and (3.23) show the plywood frame in which the slabs were casted.

Figure (3.22): Plywood Frame on which Slabs were Casted

Figure (3.23): Plywood Casting Frame after Polystyrene with Steel Mesh was Placed

The sandwich slabs were transported to the other marked location in the laboratory using an overhead crane. Each slab was placed on steel channels at marked locations in the laboratory. After placing slabs on the steel channels, PVC plastic pipes were inserted in the 2" (50mm) holes along the edges of the slabs were cut with the help of a hand saw.

In order to develop fixed boundary conditions at the slab edges, high-strength Dywidag® steel rods were inserted and pre stressed with the help of Hydraulic jack. After the slab was moved to the other location with the help of the overhead crane, the Dywidag® rods were prestressed to ensure secure fixation to the structural lab floor. Steel beams of depth 12.0"(304.8mm) were placed in the area enclosed by the Dywidag® rods. The orientation of the steel beams was random as they were used just to support the slab at the bottom. Figures (3.24), (3.25) and (3.26) show the test setup for the three sandwich slab specimens evaluated in this study.

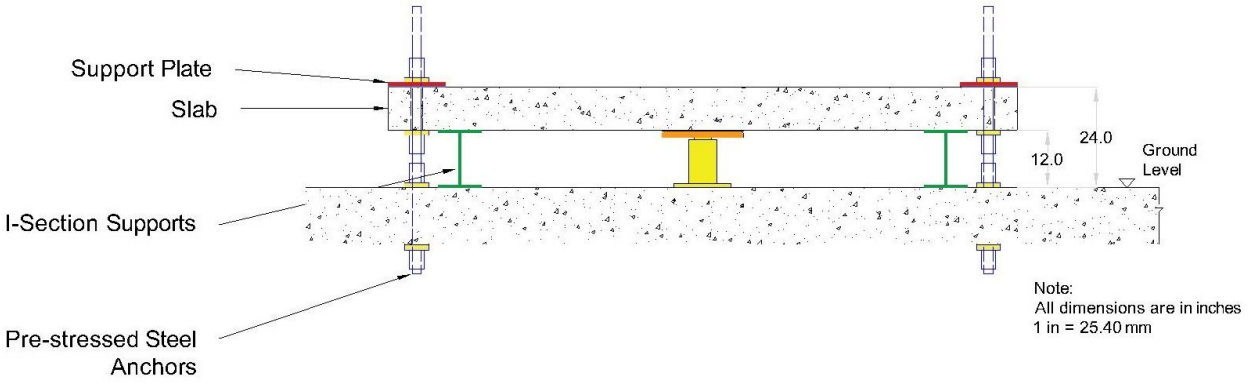

Figure (3.24): Test Setup for Sandwich Slab Specimen A

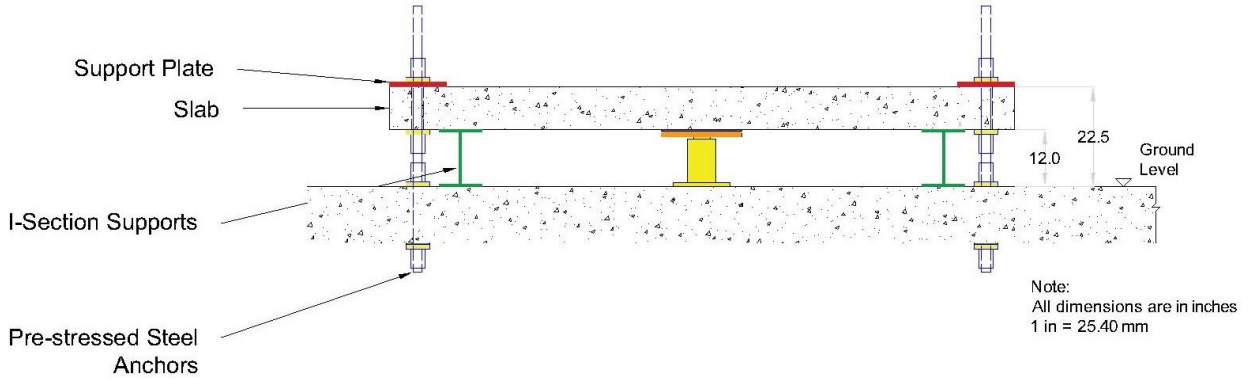

Figure (3.25): Test Setup for Sandwich Slab Specimen B

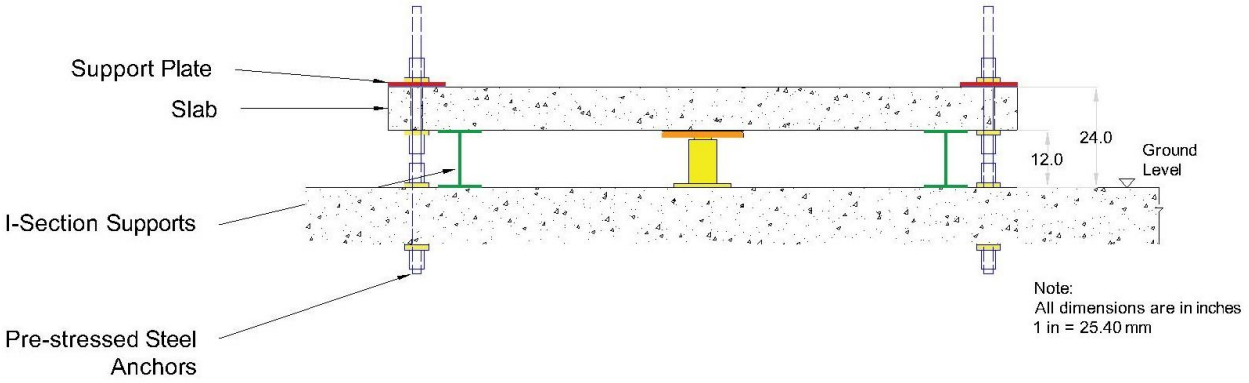

Figure (3.26): Test Set Up for Sandwich Slab Specimen C

3.4.1 Pre-stressing of Dywidag® Rods

All three sandwich slabs tested in this study were supported on four 12.0"(304.80mm) deep wide-flange steel beams prior to the start of loading to support the own weight of the sandwich slabs. The fixed boundaries were created using ¾"(19.0mm) thick A36 grade steel plates. The steel plates were fixed to the slabs with high-strength rods. For slab specimens A and B, twelve 1.5" (38mm)

diameter high-strength DYWIDAG THREAD BAR® steel rods were installed and securely fastened to the slab. For slab specimen C, the number of the DYWIDAG THREAD BAR® steel rods was sixteen with a diameter of 1.0″ (25.40 mm) that were used to fix the steel plates with sandwich slabs. In Figure (3.27), the supporting steel plates are shown in red color whereas yellow color indicates the high strength rods. The high-strength steel rods were rigidly fixed to the laboratory structural floor. The steel rods were tensioned to a stress of 4,500 psi(31,026 kN/mm^2)so that the rods are completely fixed with the slab.

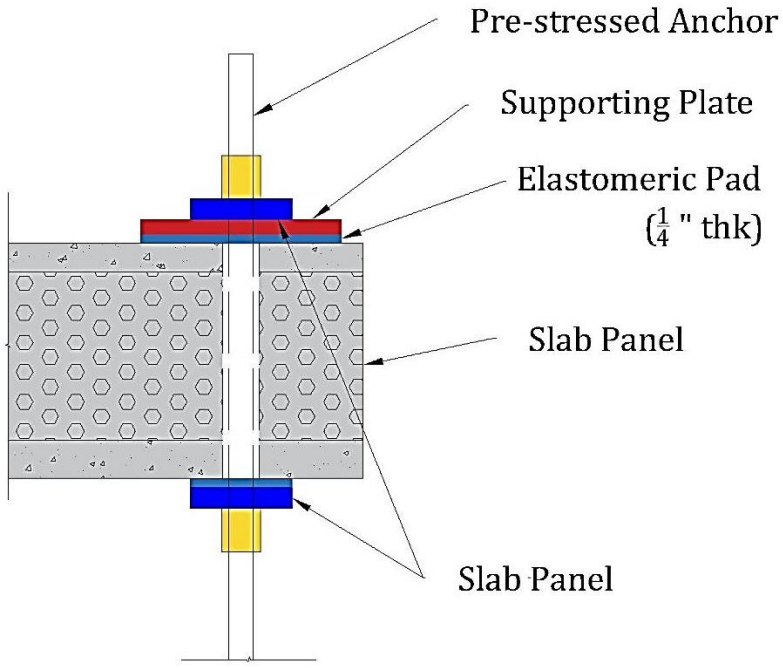

Figure (3.27): Support System for the Slab Specimens

3.4.2. Fixed Boundary Edge Conditions

The edges of all the three sandwich slab specimens were fixed and the fixed-end boundary condition was attained as follows:

i. The slab specimen was lifted using the overhead crane and was kept over the platform of steel beams and anchor plates as shown in Figure (3.28).

ii. Four steel plates 1, 2, 3, and 4 for each of the four edges of each slab were prefabricated in shop and were brought to UCI SETH laboratory.

iii. For each of the plates, holes of the diameter and center to center distance same as holes along the edges of the slab specimens were made during their fabrication.

iv. Each of the steel plates 1, 2, 3, and 4 were placed along their respective orientations along the edges of the slab specimen, such that the pre-stressed rods passed through the holes in the steel plates.

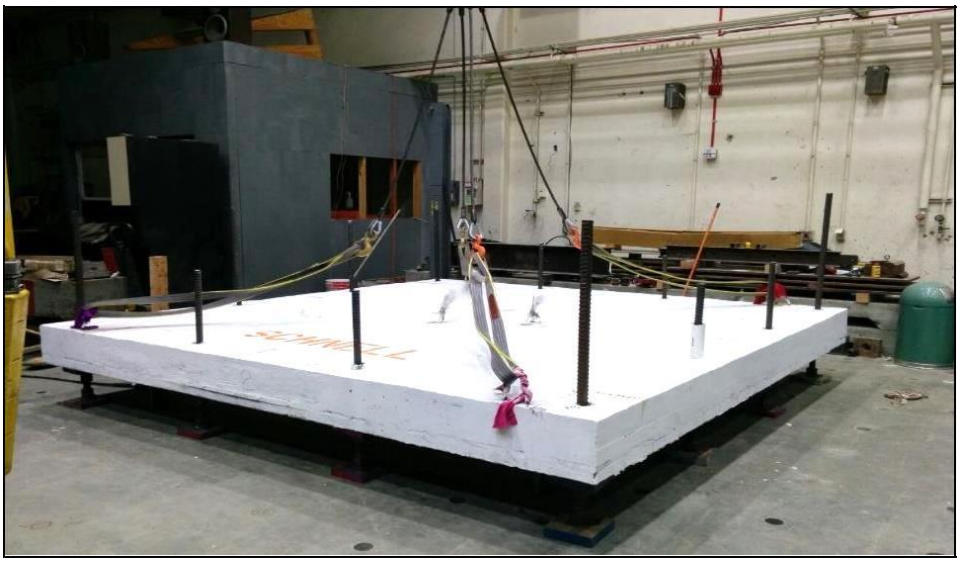

Figure (3.28): Test Setup Showing Slab Specimen Placed on Top of Steel Beams

v. Elastomeric pads of the dimensions same as the steel plates were placed between the steel plates and slab surface so as to avoid direct contact between the concrete surface and steel plates and insure uniform load distribution.

vi. The steel plates (see Figure (3.29)) were anchored with the rods with the help of anchor steel plates and nuts. The entire arrangement after placing the steel plates is shown in Figures (3.30) and (3.31).

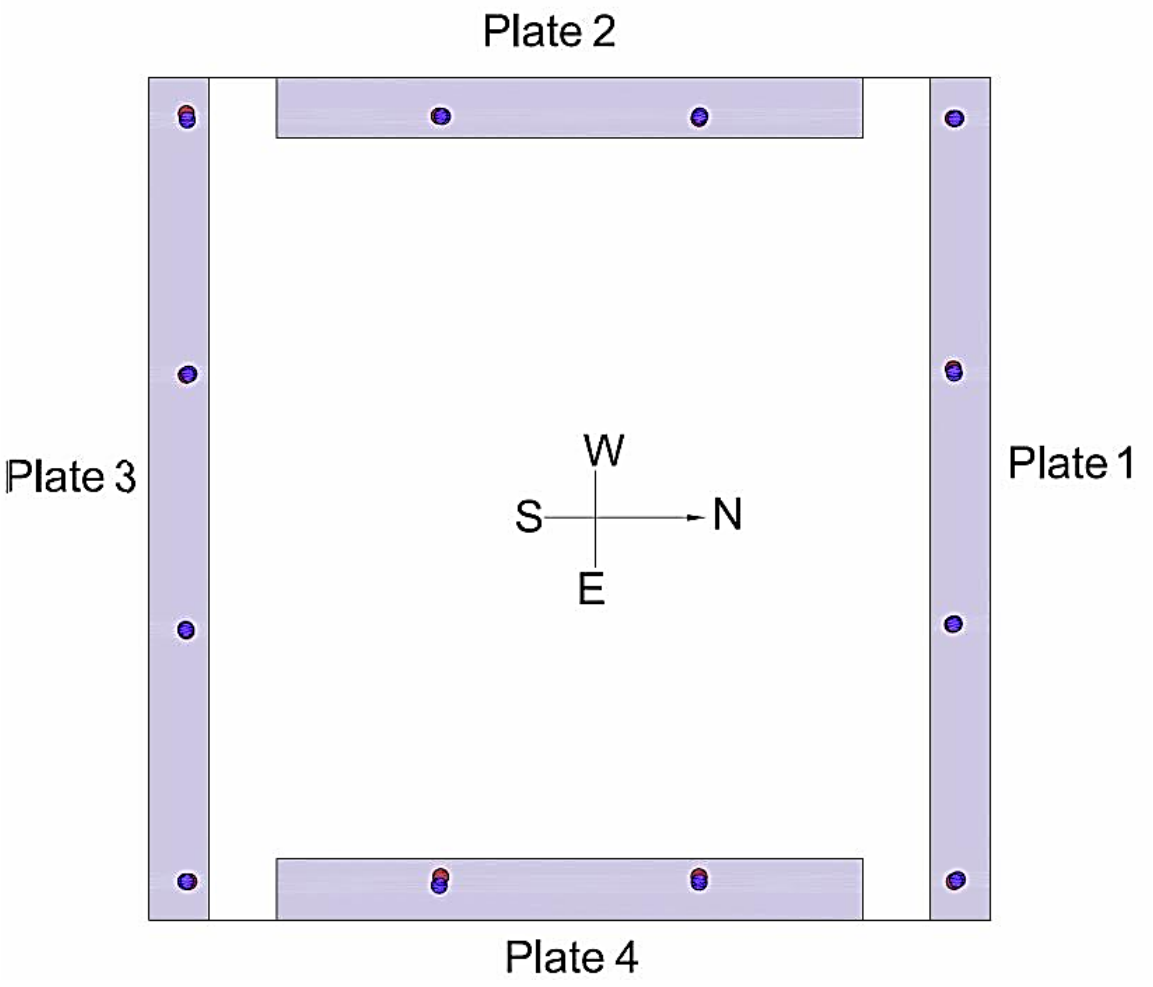

Figure (3.29): Typical Arrangement of Steel Plates on Test Specimens

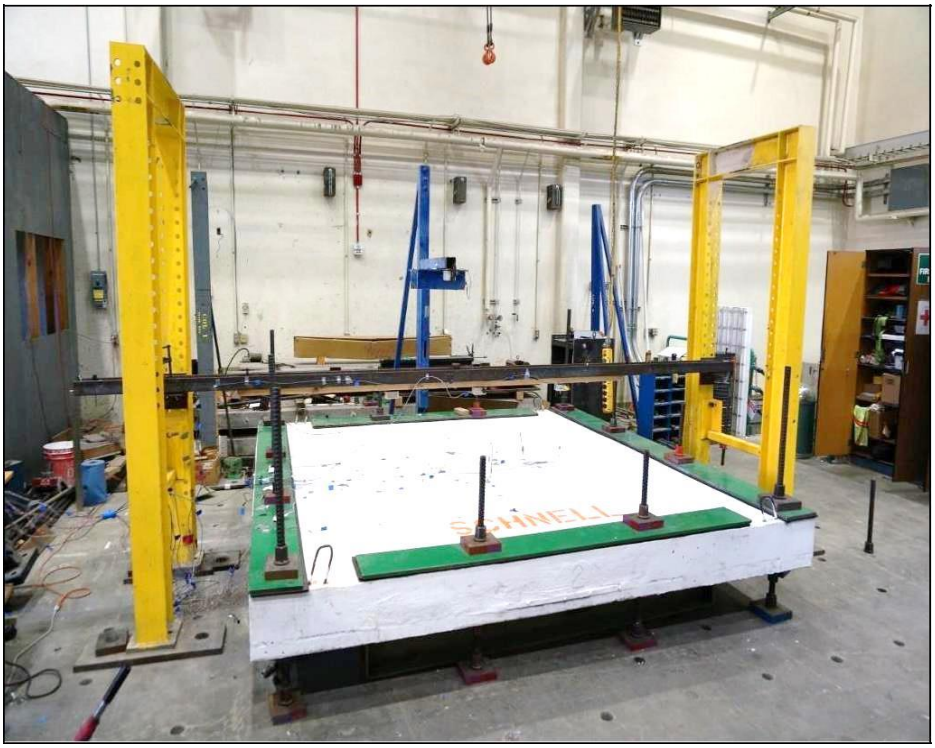

Figure (3.30): Experimental Setup for Sandwich Slabs A and B

Figure (3.31): Experimental Setup for Sandwich Slab C

3.4.3Preparation of String Potentiometer Assembly

String potentiometers were used to measure the deflection of the sandwich slab specimens. The critical points were identified and located on the top surface of each slab specimen (see Figures (3.32), (3.33) and (3.34))

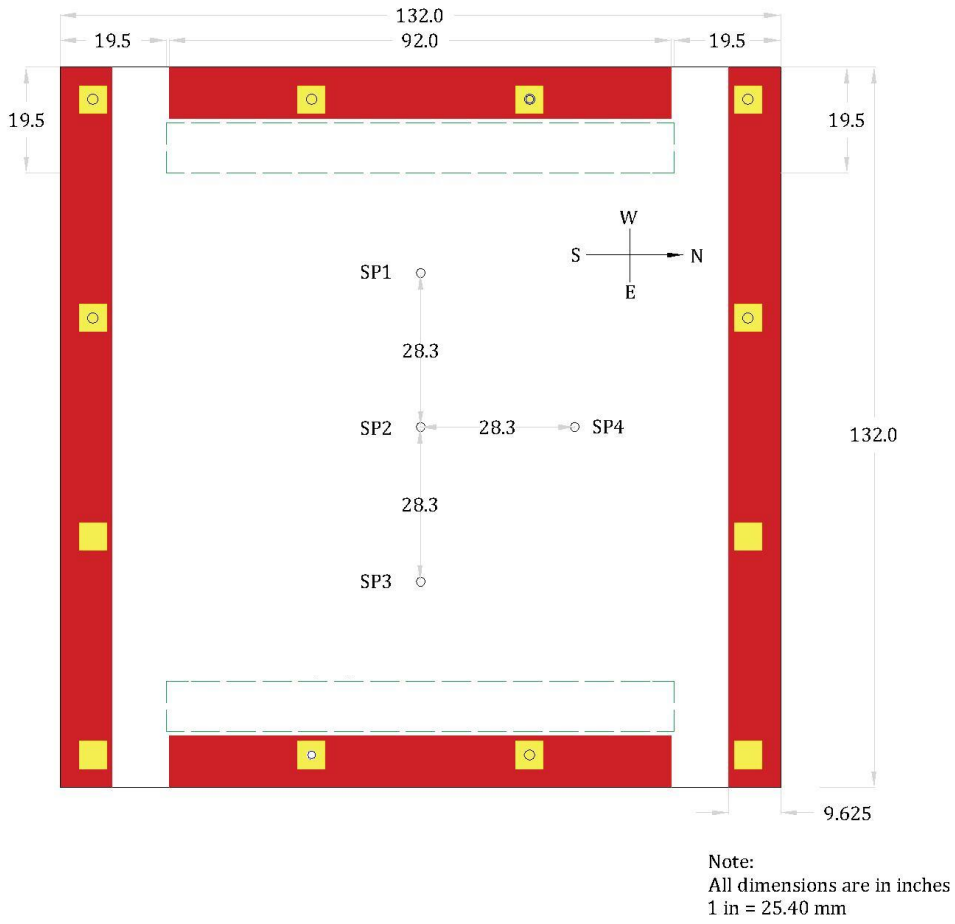

Figure (3.32): Locations of String Pots for Sandwich Slab Specimen A

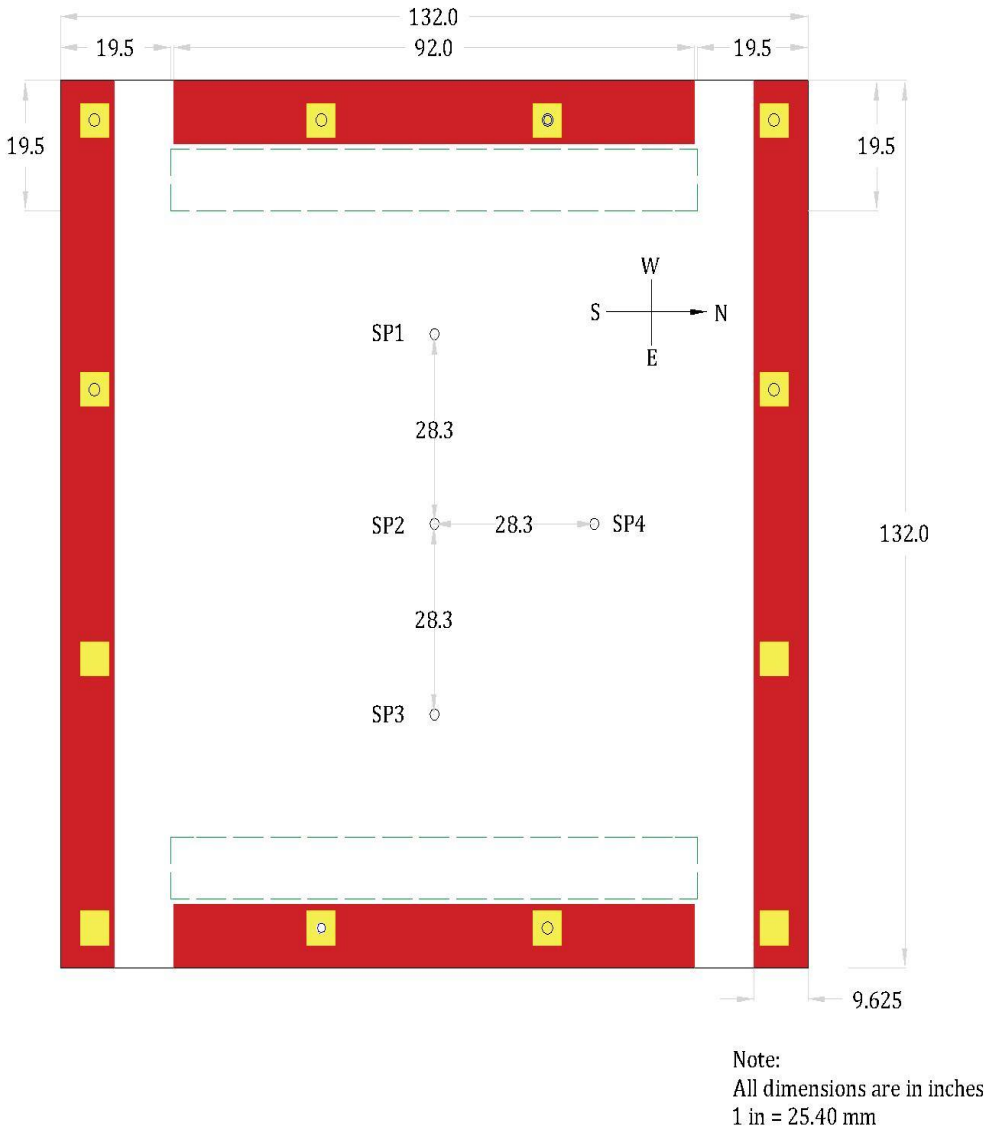

Figure (3.33): String Pots Locations for Sandwich Slab Specimen B

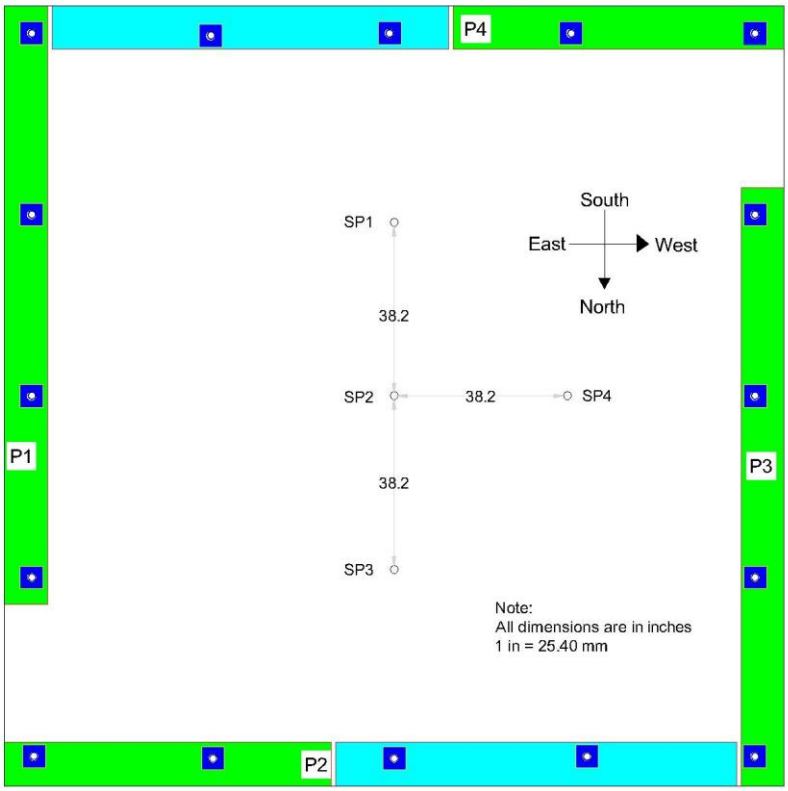

Figure (3.34): String Pots Locations for Sandwich Slab Specimen C

The entire string pot assembly was developed as described below:

i. Two yellow steel frames were placed on two opposite sides of the slab. The steel frames were kept at their respective positions with the help of the overhead crane.

ii. In between the two steel frames, one steel channel spanning across the slab was placed and fixed in between them. The arrangement is shown in Figure (3.35).

iii. The string pots SP1, SP2 and SP3 above the marked locations of slab specimen were attached to the steel channel (see Figure (3.36)).

Figure (3.35): Setup Showing Steel Channel Placed Between Steel Frames.

iii. For the string pot SP4, a blue steel angle with a cantilevered arm was placed on the third side of the slab such that the cantilevered arm spans over the position of marked location of string pot on the slab. String pot was fixed to the cantilevered arm over the marked position (see Figure 3.37).

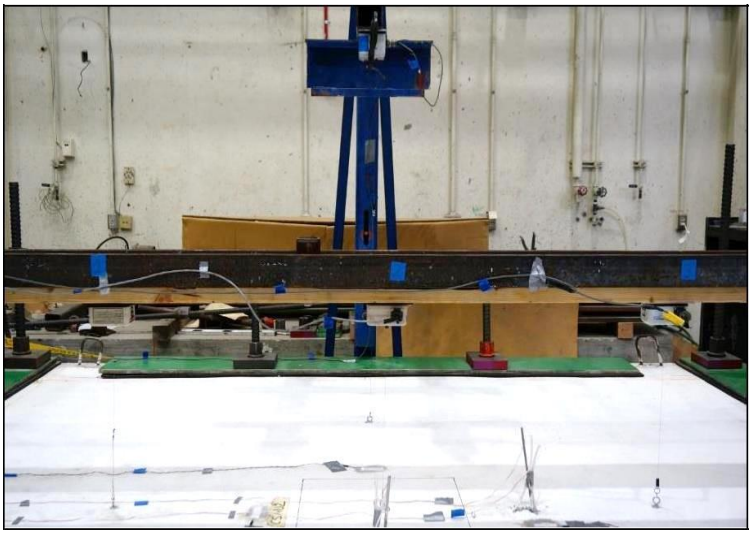

Figure (3.36): Set Up Showing String Potentiometers SP1, SP2, and SP3Attached to the Sandwich Slab Top Surface

Figure (3.37): Setup Showing String Potentiometer SP4 Mounted on a Cantilever Steel Frame

3.4.4. Test Procedure

Prior to application of out-of-plane loads on the slab specimens, both strain and defection sensors were installed at predefined positions. The experimental setup prior to the application of loads is shown in Figures (3.38) and (3.39).

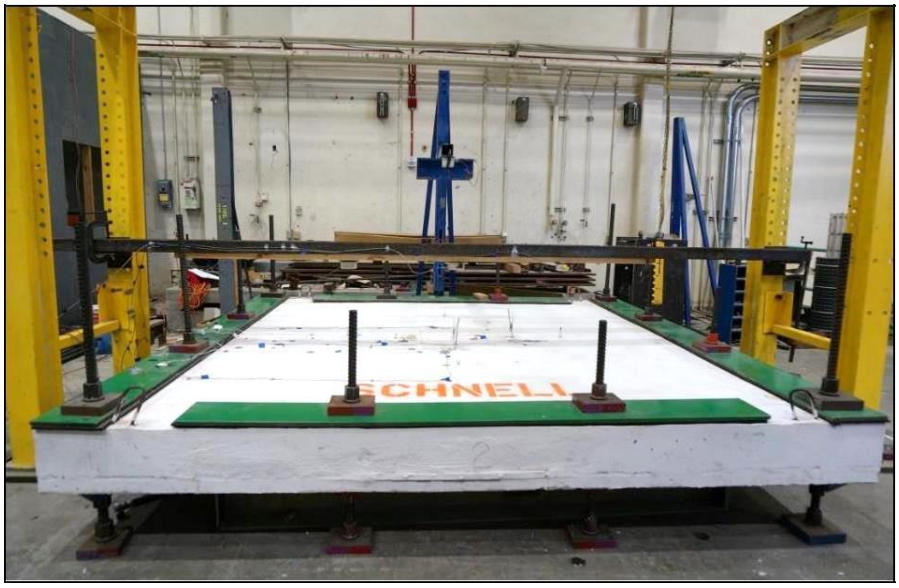

Figure (3.38): Experimental Setup for Sandwich Slab Specimens A and B

Figure (3.39): Experimental Setup for Sandwich Slab C

All instrumentation readings were taken for both loading and unloading. Throughout the loading sequence, and at each load increment, a complete set of strains and deflection measurements were recorded and stored via the computerized data acquisition system. In addition, cracks initiation and propagation as well as cracks lengths and widths were observed and recorded throughout each test. The failure mode of each slab specimen was identified and recorded. After the completion of each test, a careful inspection of cracks and locally damaged areas was performed and a crack map was developed. The detailed testing procedure of each slab specimen is described in the following paragraphs.

After slab specimen was placed on its supporting frame and preparation of entire experimental test setup, a central concentric vertical load was applied via a calibrated hydraulic jack as explained in previous chapters. As the test was load controlled, in all tests, loading rate of 3.0 psi per second (21 kN/m^2 per sec) was adopted. For each loading level, cracks were marked with the associated load level. Crackling sounds occurred during each test were recorded for further post-test analysis. The data acquisition system was recording all the strains, deflection and the load applied. When data acquisition system started showing constant deflection and applied load was decreasing, loading was stopped as slab had reached to its ultimate failure point. The duration of loading was 20 minutes and cracking pattern of slab so obtained was marked properly and for each crack its crack width was measured. The cracking pattern is shown in Figures (3.40), (3.41) and (3.42).

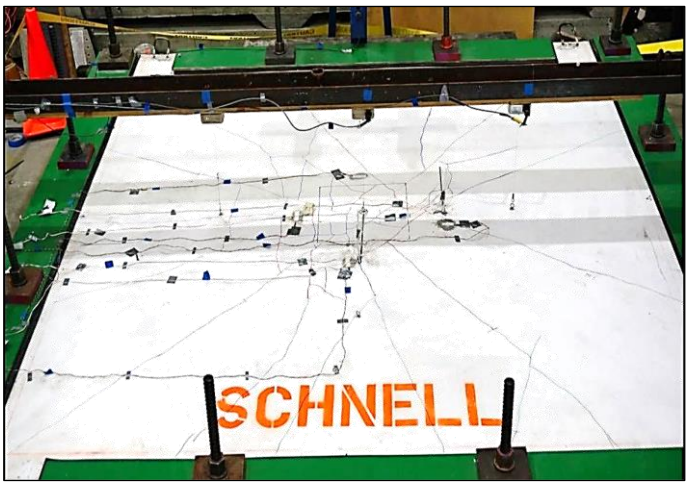

Figure (3.40): Cracks Pattern for Sandwich Slab Specimen A

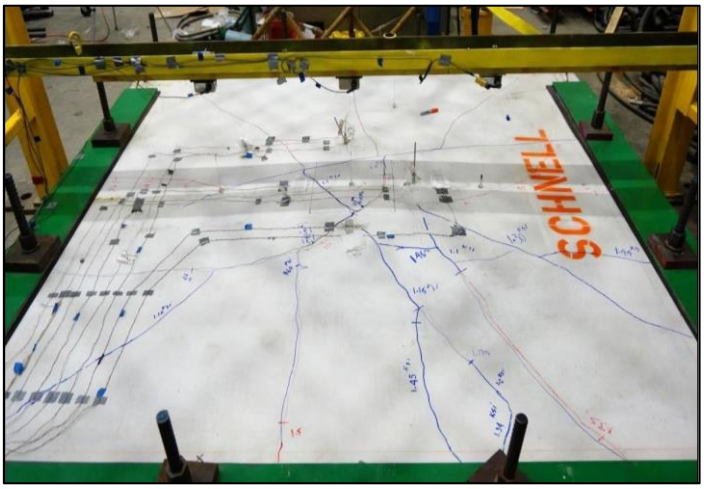

Figure (3.41): Cracks Pattern for Sandwich Slab Specimen B

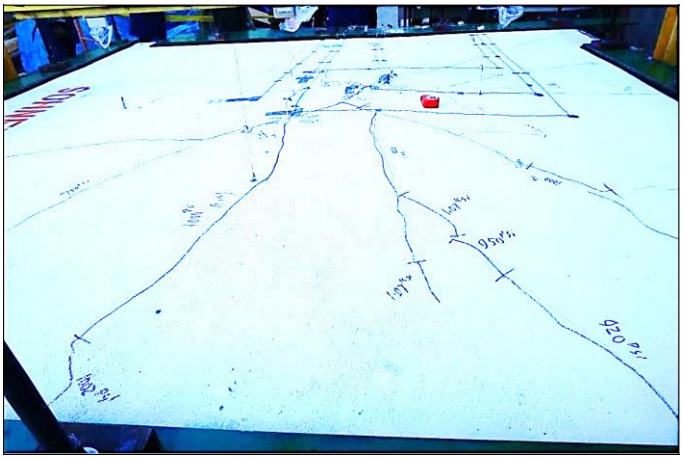

Figure (3.42): Cracks Pattern for Sandwich Slab Specimen C

3.5 Experimental Results

3.5.1<u>Sandwich Slab Specimen A:</u>Load was applied at constant rate and corresponding deflection of slab at critical points as determined by yield line theory was recorded in Data Acquisition system as described earlier. Cracks were monitored, recorded and analyzed throughout the test (refer to Figure (3.43)).

Initially, no cracks were observed. As the load increased, diagonal hair cracks that were initiated from the corners started to appear. The first observed crack on the top surface was at 7 kips (31kN).The behavior was linear up to about 10 kips (44.8kN), after which a nonlinear stiffness degradation was observed as the size and width of the cracks increased beyond the 10kip (44.8kN) load level as shown in Figure (3.43). The first cracking sound was occurred at 7 Kips (31kN). As the load increased beyond 15.0 kips(66.72kN), more diagonal and transverse cracks were developed that caused stiffness degradation as depicted in Figure (3.43). Figure (3.45) shows the distribution and density of cracks at the central loading area. The maximum equivalent total load capacity of this 2way-slab specimen was 22.0 kips (97.86 kN) with a corresponding central mid-span deflection of 2.41″ (61.2mm) as shown in Figure (3.44). The loading was halted as the cracks width increased to unusable value (see Figure (3.45)) up to 1" (25.4mm). The ultimate failure of the specimen was identified as a tensile flexural failure. Figure (3.47) present the Load vs. Strain relationship for Steel Wires .

Figure (3.43): Cracks were Monitored, Recorded and Analyzed throughout the Test

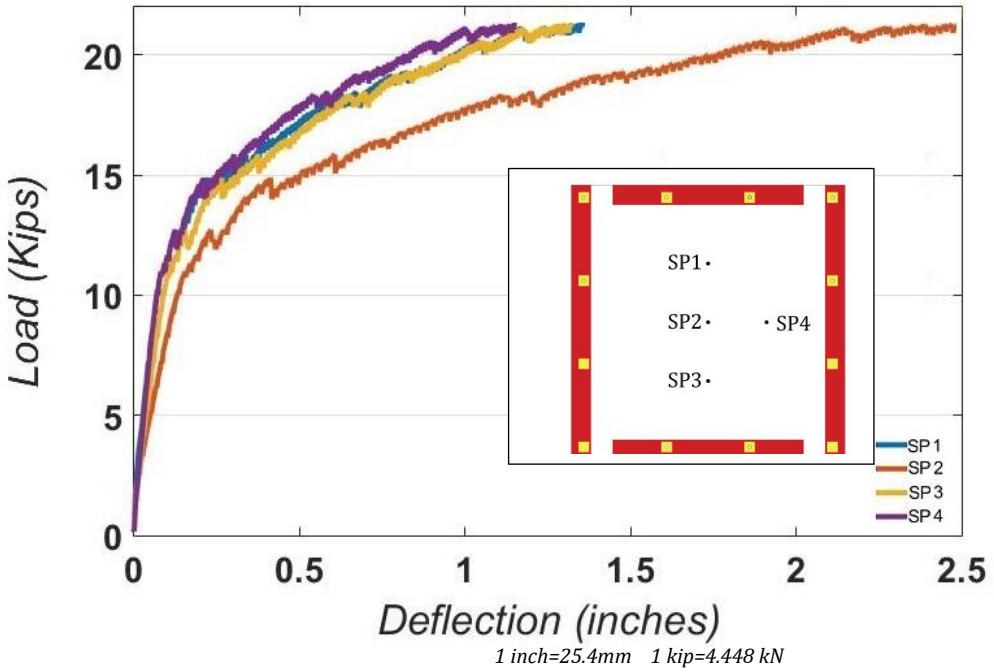

Figure (3.44): Load-Deflection Curve for Sandwich Slab Specimen A

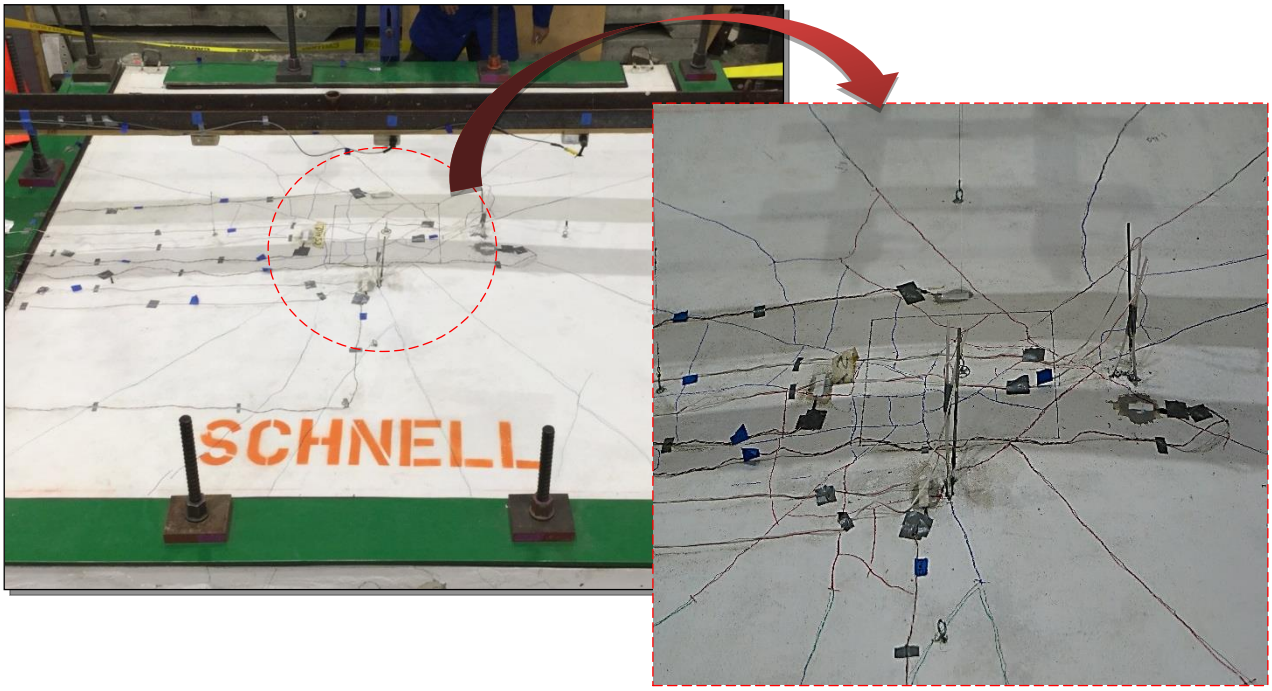

Figure (3.45): Distribution and Density of Cracks at the Central Loading

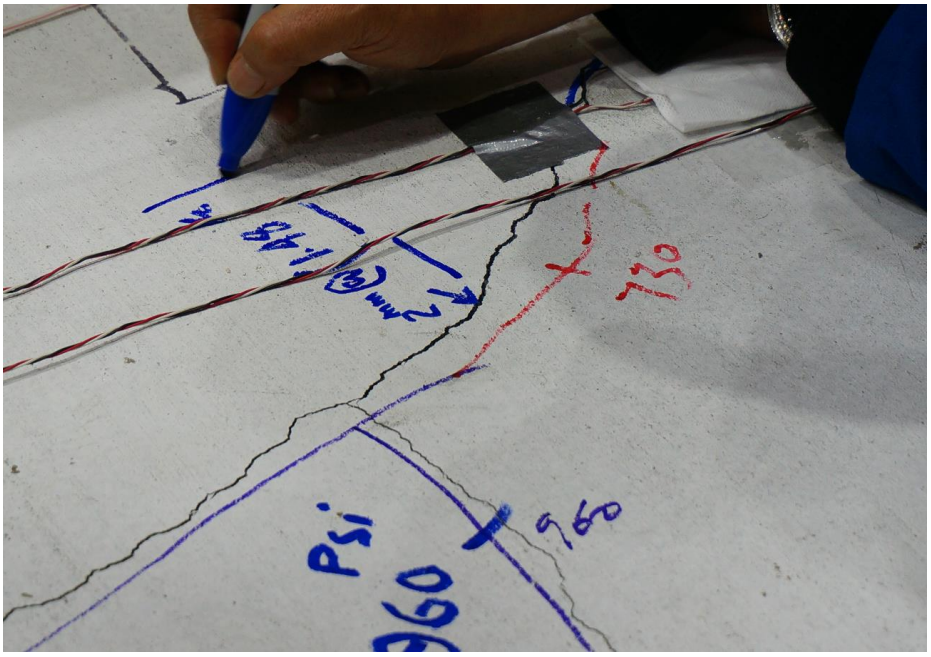

Figure (3.46): Large Cracks Widths at Central Loading Area of Sandwich Slab A

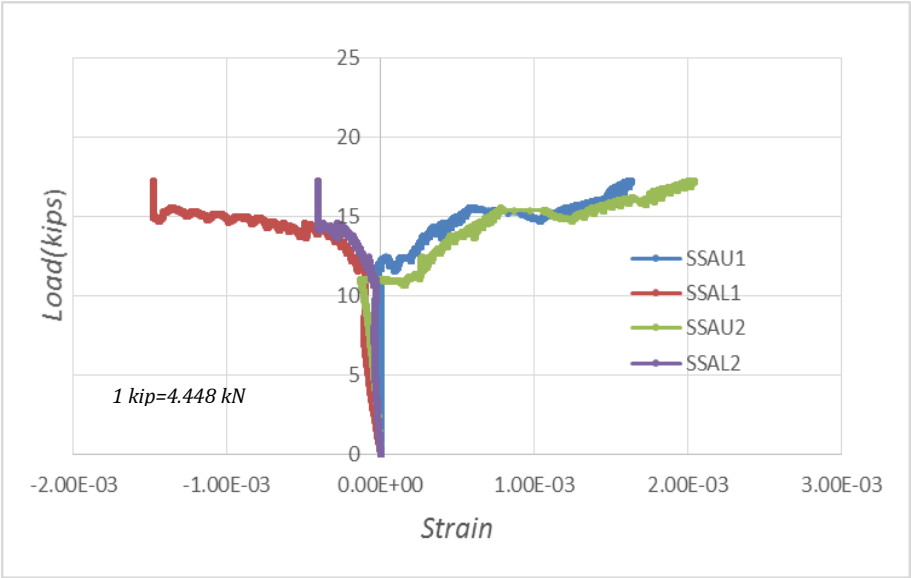

Figure (3.47): Load vs. Strain relationship for Steel Wires

3.5.2<u>Sandwich Slab Specimen B</u>: Similar setup and loading protocol to specimen A was adopted. Cracks initiation, propagation and size growth was identified and recorded throughout the test (refer to Figure (3.48) and Figure (3.49) for the load-deflection curve of this specimen). As expected the deflection at the central location was higher than those at 1/3 span locations. Similar trend was observed for the load-deformation behavior, however, the non-linearity was developed at a slightly lower load level of about 6.0 kips (26.7kN). As the load increased, cracks appeared on the top tensile surface of the sandwich specimen as shown in Figure (3.50).The first cracking sound occurred at 6.0 Kips (26.7kN). As out-of-plane load increased, more cracks were developed and the size of the existing cracks were enlarged up to 0.10" (2.5mm) at a load level of 18.8 kips (83.6 KN)as shown in Figure (3.51). The ultimate load for this specimen was 20 kips (89kN) and the mode of failure was identified as flexural tensile

failure with large cracks size. Figure (3.52) presents the load-strain curve for steel wires of sandwich specimen B.

Figure (3.48): Cracks Initiation, Propagation and Size Growth were monitored throughout the Test

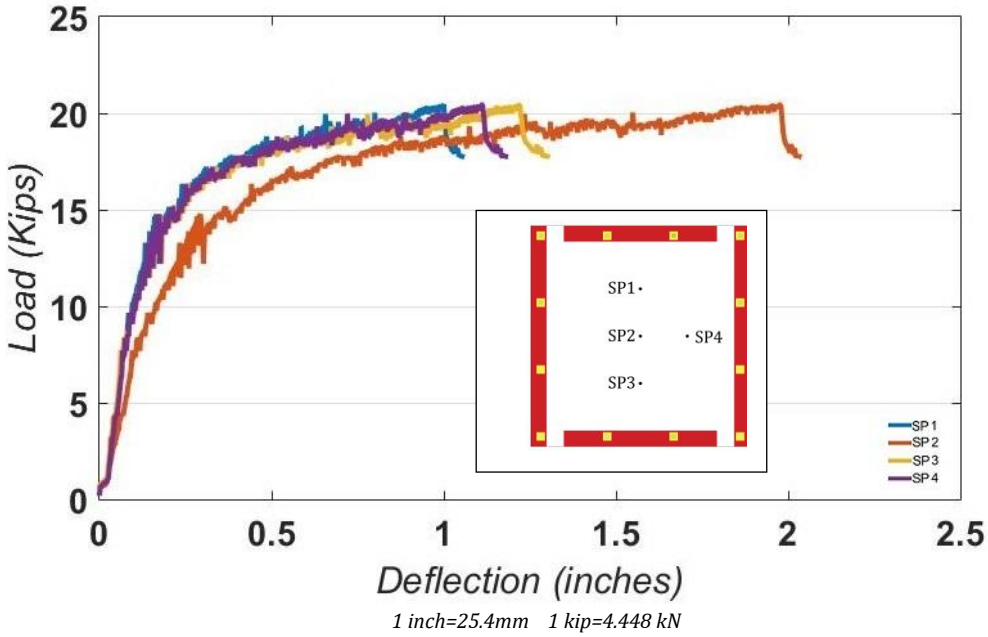

Figure (3.49): Load-Deflection Curve for Sandwich Slab Specimen B

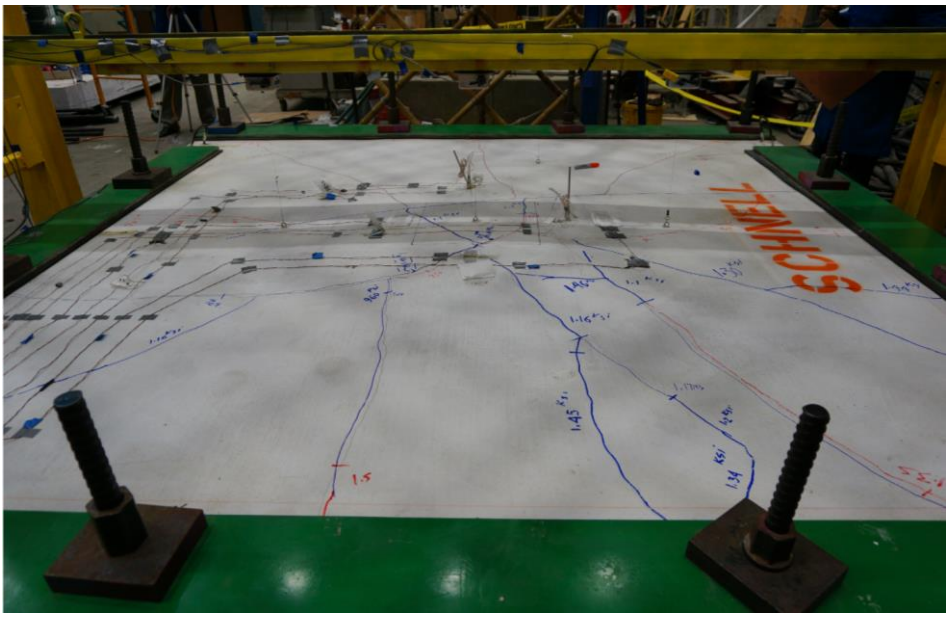

Figure (3.50): Development and Propagation for Sandwich Slab B

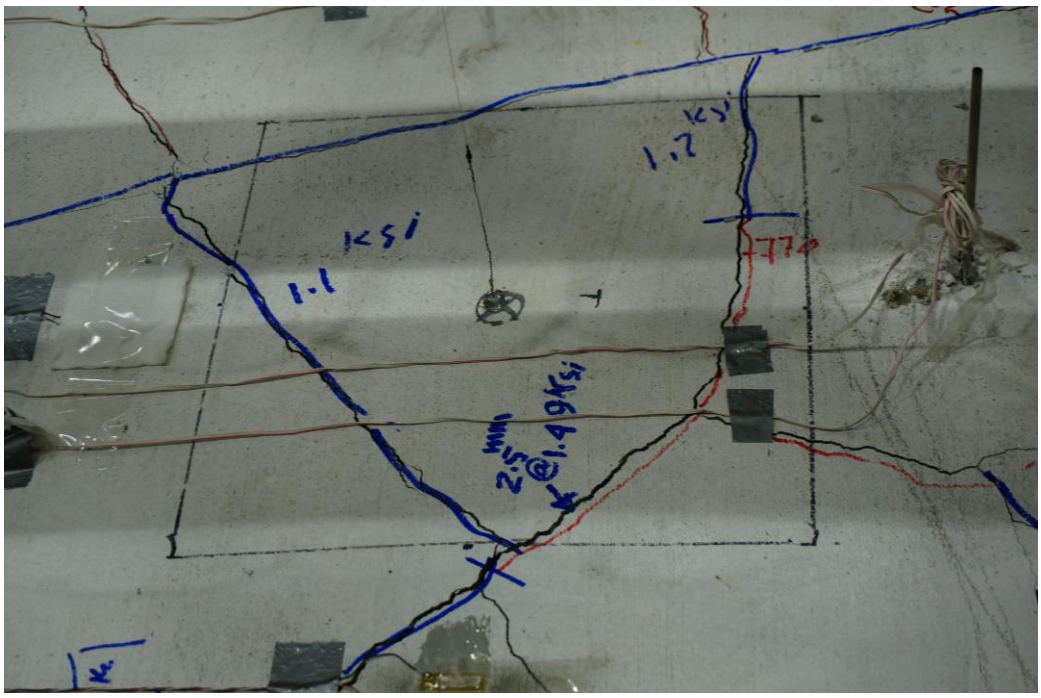

Figure (3.51): Increase of Size of Cracks at Higher Out-of-Plane Load

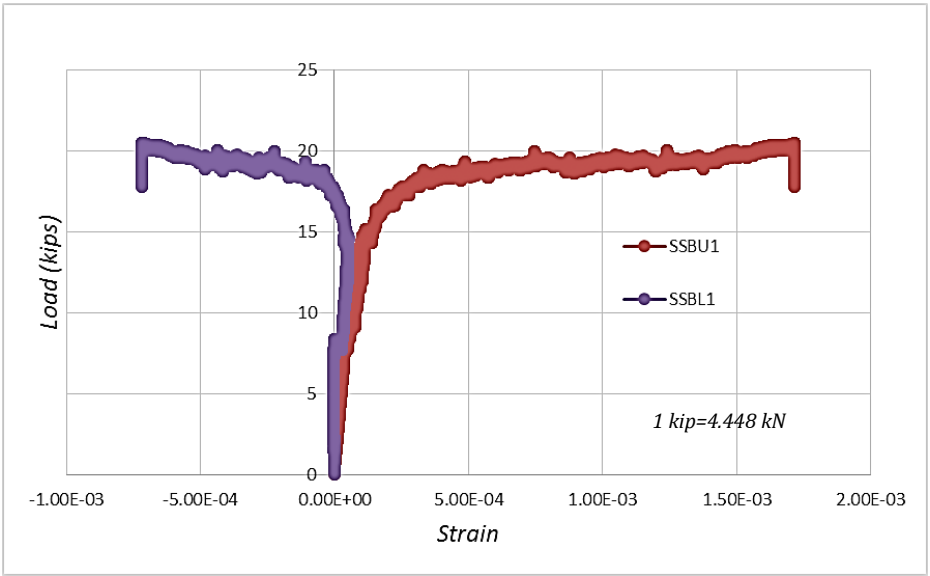

Figure (3.52) Load-Strain Curves for Steel Wires of Sandwich Specimen B

***3.5.3*Sandwich Slab Specimen C:** This sandwich slab specimen was larger in dimensions as compared to slab specimens A and B for which the overall dimension was 4.0m x 4.0m (172.0"X 172.0") and with a total thickness of 300mm (≈12.0"). Due to the large size and weight of this specimen that was fabricated outside the covered area of the laboratory, it was impossible to transport the specimen inside the lab. A decision was made to conduct the test for this large-scale specimen in the outdoor area of SETH laboratory.

Similar test setup (see Figure (3.53)) and loading protocol was adopted for this specimen. Initially and up to a load level of 4.2kip(18.7KN) no cracks were observed on the top tension side of the slab. At a load of 4.2kip (18.7KN), the first diagonal crack was initiated from the center of the slab as shown in Figure (3.54).

Figure (3.55) presents the load-deflection curves for different locations of the slab. As shown in this figure, the linear behavior ended at a lower level as compared to other two sandwich slabs and non-linearity started at a load of 5.0kips (22.24kN). At this load level, a slight stiffness degradation was observed due to accumulation of cracks at the tension side of the slab specimen. Appreciable stiffness degradation occurred at a load of 10.50kips (46.70kN) that continued until the end of the test. Figure (3.56) shows the cracks distribution of the sandwich slab "C". The load-strain curve for steel is presented in Figure (3.57).

Figure (3.53): Test Setup for Sandwich Slab Specimen C

Figure (3.54): First Hair Crack on the Tension Top Side of Sandwich Slab Specimen C at a Load Level of about 6.0 kips (26.7kN)

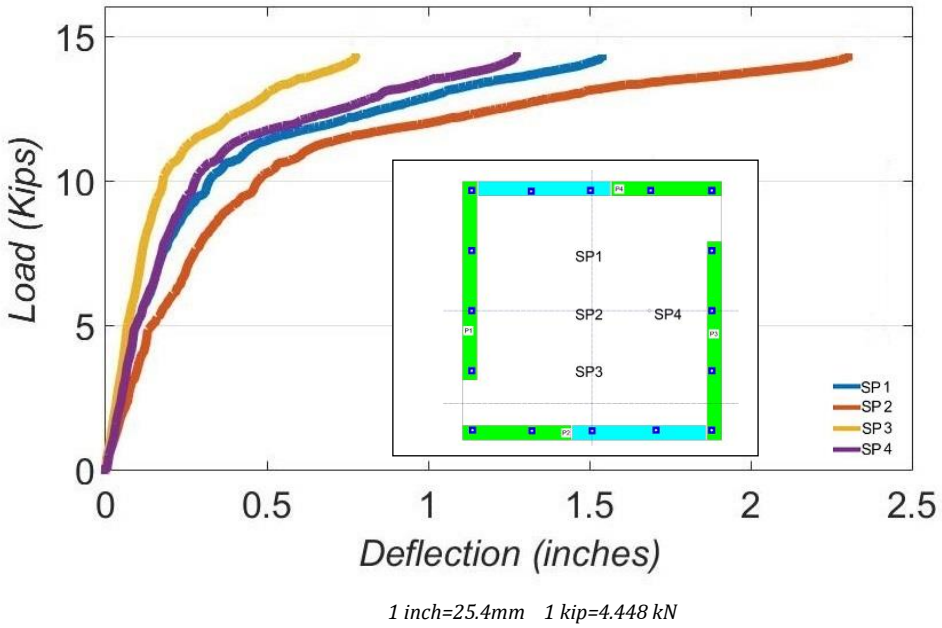

Figure (3.55): Load-Deflection Curve for Sandwich Slab Specimen C

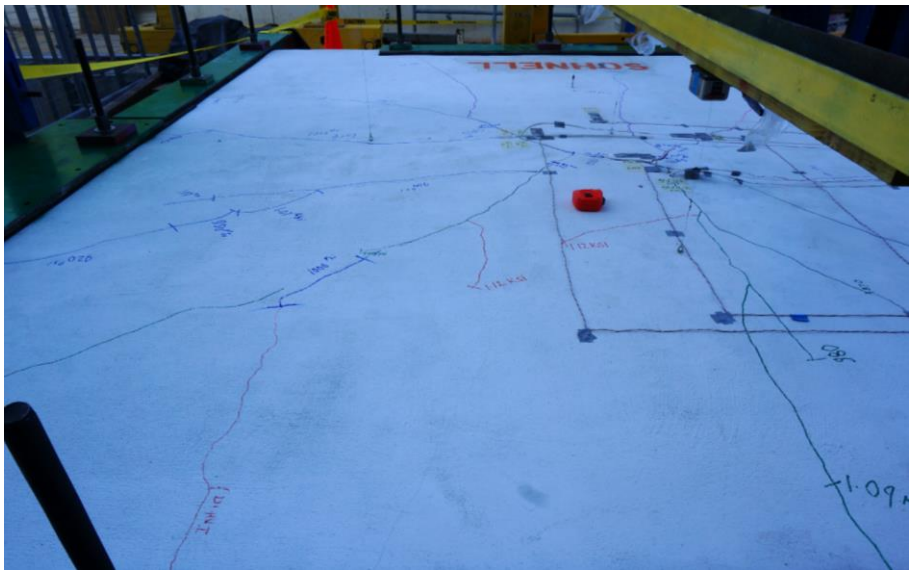

Figure (3.56): Cracks Distribution of Sandwich Slab Specimen C

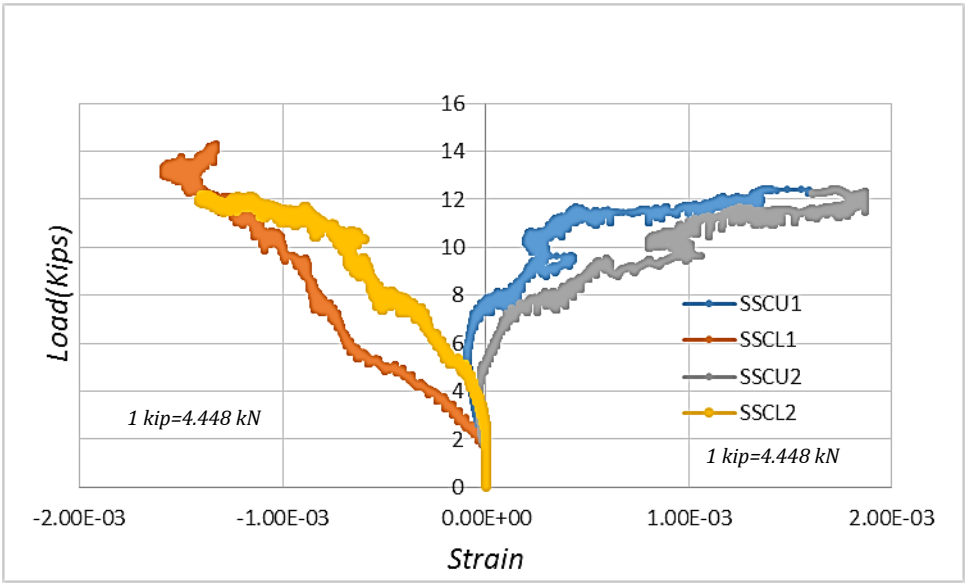

Figure (3.57): Steel Strain Curve for Slab Specimen C

3.5.4Summary of Results

From the strain gages bonded to the top mortar surfaces it was observed that as the cracks increased in both width and length, a decrease in flexural stiffness was noticeable. The cracking and ultimate loads for the three specimens are summarized in Table (3.8).

Table (3.8): Maximum and cracking Experimental Load for Sandwich Slab Specimens

Slab Specimen ID	Maximum Load (P_{max}) kN[kips]	Cracking Load (P_{cr}) kN[kips]
A	98.0 (22.0)	31 [7.0]
B	90.0(20.0)	26.7[6.0]
C	62.3 (14.0)	18.7[4.2]

3.5.4.1 Load-Strain Behavior:

The strain gages that were bonded to steel wires were labeled as SSAU1, SSAU2, SSAL1, SSAL2, SSBU1, SSBL1, SSCU1, SSCU2, SSCL1, SSCL2. Steel-strain curves for slab specimens are shown in Figures (3.39), (3.45), and (3.50). Table (3.2) shows the vales of steel wire strain in tension side of the slab at the maximum load.

Table (3.9): Steel Wire Strain in Tension Side at the Maximum Load

Slab Specimen	**Maximum Load kN (kips)**	**Steel Wire Strain**
A	98.0 (22.0)	0.0021 (yield occurred)
B	90.0(20.0)	0.0018 (yield did not occur)
C	62.3 (14.0)	0.0019 (yield occurred)

CHAPTER 4

ANALYTICAL VERIFICATION USING ACI 318 CODE

In this chapter, a simplified analytical procedure following the provisions of the American Concrete Institute ACI 318-14 is adopted to predict the ultimate strength and deflection of the sandwich slabs evaluated experimentally in this study. In addition, a comparison between the analytical and the experimental results is performed in order to verify the validity of the modified ACI procedures.

4.1 Theoretical Analysis of Sandwich Slab Specimens

This section provides the estimation of the moment capacity of the sandwich slabs evaluated experimentally in this investigation using ACI 318-14 code procedures. Following are the important assumptions used in this analysis:

i) A full composite action is achieved which means it is assumed that the parallel wire shear connectors have enough shear capacity to carry shear forces transmitted across the sandwich slab section.

ii) The composite section remains plane after bending, i.e., it follows Bernoulli's bending theory.

iii) The strength of the EPS foam core is neglected, and does not contribute to the strength of cross section.

iv) The average thickness of concrete is considered over the polystyrene and change in thickness of concrete is because of wavy geometry of the EPS foam.

v) The contribution of the compression steel is neglected, i.e., the section is treated as a singly-reinforced section under bending.

vi) The neutral axis (NA) lies at the contact location of mortar and the expanded polystyrene foam core. This imposes a limitation that the NA can only be located in the compression shell of the sandwich slab.

Figure (4.1) shows the strain distribution in the cross section based on the second assumption stated earlier. It also shows the free body diagram for cross section of EPS concrete panel under bending.

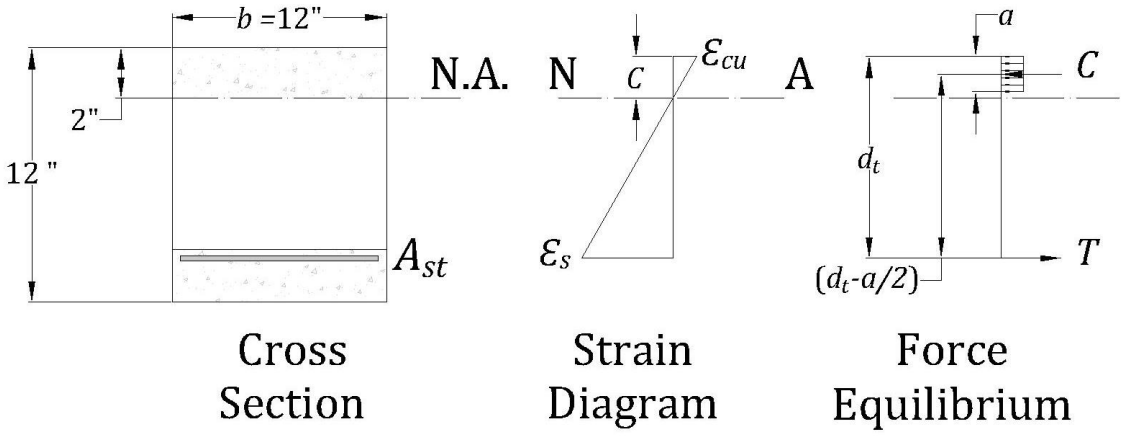

Figure (4.1): Strain Variation and Force Equilibrium for the Sandwich Slab Cross Section Subjected to Flexure

4.1.1 Analytical Calculations of Slab A

4.1.1.1 Flexure Analysis

Concrete strength: f'_c= 33,750kN/m^2 (4,895 psi) ,

$\beta_1 = \frac{0.05(f'_c - 4000)}{1000} = 0.80$ (ACI 318-14 Table 22.2.2.4.3b)

Yield strength of steel: f_y= 3,86,106kN/m^2 (56,000 psi) at ε_{sy} = 0.00206

Clear span = slab width – 2* plate support at each side =132.0– 2x9.5 = 2.87 m(113 in)

No. of steel wires along the width in the direction where the wire spacing is 3.15" = 113/3.15 = 36 wire

Diameter of one steel bar, d_b = 3 mm (0.1180)''

A_s for one steel bar = 0.0110 in^2

Total tension steel area, A_s =*255 mm^2(*0.396 in^2)

Modulus of Elasticity for steel = E_s=20 x 10^{10}kN/m^2(2.9 x 10^9 psi)

Assume C = the thickness of the concrete layer under compression = 51 mm (2.0 in)

The depth of Whitney stress block is found as,

$a = \beta_1 c = 0.80\ x\ 2.0 = 41\ mm$ (1.60 ")

For 12'' thick slab, the effective depth for tension steel is, d_t = (12 – 1.5 – 0.118/2) =265 mm (10.44 “)

The strain in steel can be determined by similar triangle method as shown below,

$$\frac{\varepsilon_s}{(d_t - c)} = \frac{\varepsilon_{cu}}{c} \qquad (4.1)$$

$$\frac{\varepsilon_s}{(10.4410 - 2.0000)} = \frac{0.0030}{2.0000}$$

$\varepsilon_s = 0.0126 > \varepsilon_y = 0.0021$

Hence, the assumption that the steel has yielded in tension is correct. The nominal moment capacity of the cross section is given by,

$$M_n = A_s f_y \left(d_t - \frac{a}{2}\right) \qquad (4.2)$$

$M_n =$ 0.396 x 56 x $(10.4410 - \frac{1.6}{2})$

$M_n =$ 213.8kip-in = 24 kN-m (17.82 kip-ft)

But;

$$M_n = 0.5\frac{pl}{4} - 0.5\frac{wl^2}{8} \qquad (4.3)$$

where;

P=concentrated load applied in the center line of the slab, and as the slab is rectangular, the distribution factor for transferring load in two directions is 0.5.

W=own-weight of the slab which is acting (downward) in the opposite direction of the applied load (upward), and as soon as the slab is rectangular then the distribution factor for transferring load in two directions is 0.50.

$$w = \text{specific weight of the slab} * \text{weidth} * \text{thickness} = \frac{145}{12 * 12 * 12} * 113 * 3.5$$

$$= 592 \frac{kg}{m} (33.19 \frac{lb}{in})$$

$$17.82 * 12 * 1000 = \frac{0.5\ P_n * 113}{4} - 0.5 * 33.19 * \ (113)^2/8$$

$$P_n = 76kN\ (17.0\ kips\ )$$

4.1.1.2 Shear Analysis

The nominal shear strength shall be calculated ignoring the shear connectors contribution and taking into account only the thickness of concrete layer in tension side.

$$v_n = 2\sqrt{f'_c}\ b\ t = 2\ \sqrt{4895} * 113 * 1.5 = 105\ kN\ (23.7\ kips) \quad \textit{ACI-318 14 Eq. 22.5.5.1}$$

but;

$$v_u = 0.5\ p/2 - 0.5\ wl/2 \qquad (4.4)$$

where:

p=concentrated load applied in the center line of the slab, and as soon as the slab is rectangular then the distribution factor for transferring load in two directions is 0.5.

W=own-weight of the slab which is acting (downward) in the opposite direction of the applied load (upward), and as the slab is rectangular, the distribution factor for transferring load in two directions is 0.50.

$$\text{w} = \text{specific weight of the slab} * \text{width} * \text{thickness} = \frac{145}{12 * 12 * 12} * 113 * 3.5 = 33.19\ lb/in$$

$$v_u = v_n = 23.7 * 1000 = 0.5\frac{p}{2} - 0.5 * 33.19 * 113/2$$

$$P_n = 4{,}38kN\ (98.55\ kips)$$

4.1.1.3 Two-Way Shear (Punching Shear) Analysis

The slab will also be susceptible for two-way shear at the location of loading plate as there is a possibility that the loading plate itself may punch through the small thickness of concrete before actually reaching the actual flexural load. Hence, it is important to estimate the punching shear capacity of the slab and compare it with failure load under flexure. Figure (4.2) shows critical section for punching for slab. As the weak polystyrene core is embedded in between concrete layers, the loading plate is likely to punch through the concrete layer in contact. Hence, considering 2.00" (50mm) thick concrete slab, punching shear capacity for slab is estimated as per ACI 318-14.

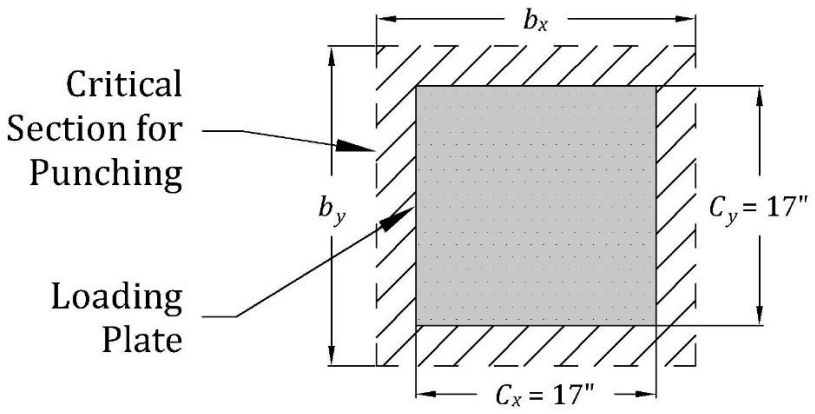

Figure(4.2): Critical Perimeter for Punching

Slab effective depth (d_{eff}) = compression side concrete - half of bar diameter = 1.9410''

$b_x = C_x + d_{eff}$ = 18.941'' and $b_y = C_y + d_{eff}$ = 481 mm (18.94'')

b_o = 2 x (b_x + b_y) =1924 mm (75.7640'')

$A_c = b_o$ x d_{eff} = 94838 mm^2 (147.0579 in^2)

α_s = 40 (assuming interior column condition)

$\beta_o = b_o / d$ = 37 and β_c = 1

ϕ = strength reduction factor = 0.75

Shear factor is considered minimum of the following:

S-Factor$_o$ = 2 + (α_s / β_o) = 3.08

S-Factor$_c$= 2 + (4 / β_c) = 6.0

S-Factor$_{max}$ = 4.0

S-Factor$_{controlled}$ = 3.08

v_n= S-Factor$_{controlled}$ ($\sqrt{f_c'}$) = 1486 kN/m^2 (215.50 psi)

The ultimate punching shear strength is computed as,

V_u= v_nx A_c= 215.5 x 147.0579 = 141kN (31.7 kips)

Hence, flexural load capacity is lesser than the shear load capacity and punching load capacity. From the experimental observations, it can be confirmed that slab specimens have flexural failure as dominant failure mode and not the shear failure and punching failure.

4.1.1.4 Theoretical Deflection

Specific weight of concrete used w = 2323 kg/m^3 (145 pcf)

F'$_c$ =33750kN/m^2 (4895 psi)

E = 33 w$^{1.5}\sqrt{f_c}$ = 277 x 10^{5}kN/m^2 (4.03 x 10^6 psi)

$$G = \frac{E}{2(1+\nu)} = 1.679x10^6$$

Clear Span L = 2870 mm (113 in)

Panel Width = 1219 mm (48 in)

Center of gravity from the bottom line of the cross section, y is given as:

$$y = \frac{I_{top} \times y_{top} + I_{bottom} \times y_{bottom}}{I_{top} + I_{bottom}}$$

y = 103 mm (4.04 in)

$I_{gross} = I_{top} + I_{bottom} + A_{top}7.21^2 + A_{bottom}3.04^2$

I_{gross} = 119 x 10^7 mm^4 (4674 in^4)

$I_{eff} = (0.2)I_{gross}$

I_{eff}= 39 x 10^7 mm^4 (935 in^4)

The slab is rectangular so the distribution factor is 0.5,

Basic deflection at the center of the panel in one direction, assuming hinged at both ends is given by:

δ = Flexure deflection + Shear deflection

$$\delta = \frac{0.5PL^3}{48EI_{eff}} + \frac{0.5PL}{4GAK_V}$$

Where;

P= Total applied load

E = concrete young's modules

I_{eff} = $0.20I_{gross}$

G = shear modulus

A = cross section area

K_v = the modified shear correction factor (Bank and Bednarczyk 1988)

$$K_v = \frac{A_{web}}{A_{gross}}$$

@ 48 in width we have six shear connector wires of diameter 0.118 in and with height of 8.5 in.

$$K_v = \frac{A_{web}}{A_{gross}} = \frac{(6)(0.118)(8.5)}{(6)(0.118)(8.5) + (48)(3.5)} = 0.034$$

$$\delta_{one\ direction} = \frac{(0.5)(P)L^3}{(48)(E)I_{eff}} + \frac{(0.5)(P)L^3}{(4)k_w(G)}$$

The total deflection at the center can be computed by the summation of the deflection in both sides, but the slab is rectangular then total deflection will be twice the deflection in one direction:

$$\delta_{Total} = 2\left[\frac{(0.5)(P)L^3}{(48)(E)I_{eff}} + \frac{(0.5)(P)(L)}{(4)K_v(G)(A)}\right]$$

$$\delta_{Total} = 7.97 \times 10^{-3}P + 3 \times 10^{-3}P(4.5)$$

where: P is in (kips) and δ is in (inch)

Using Equation (4.5), theoretical-load deflection relationship can be plotted and compared to the experimental results as shown in Figures(4.3), (4.4) and (4.5).

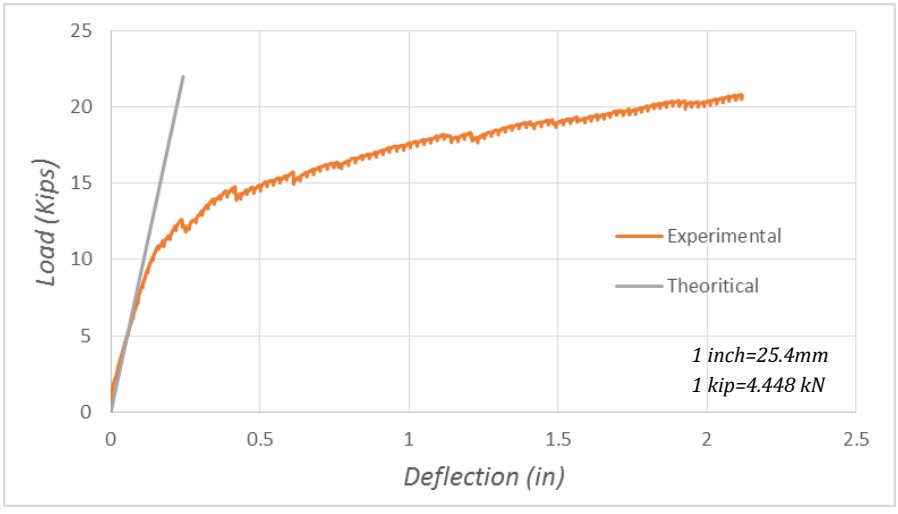

Figure (4.3): Comparison of Experimental and Theoretical Deflection for Slab Specimen "A"

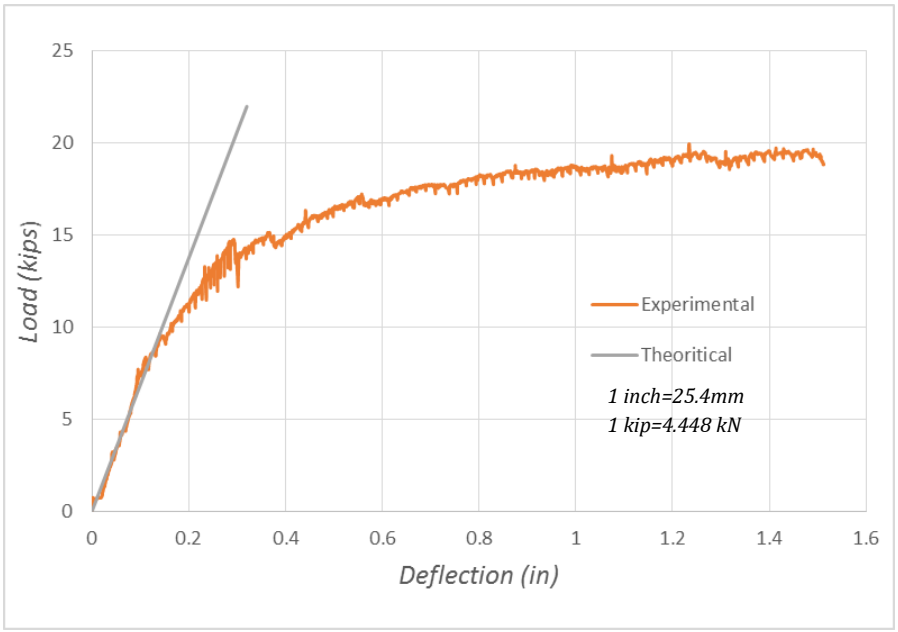

Figure (4.4): Comparison of Experimental and Theoretical Deflection for Slab Specimen "B"

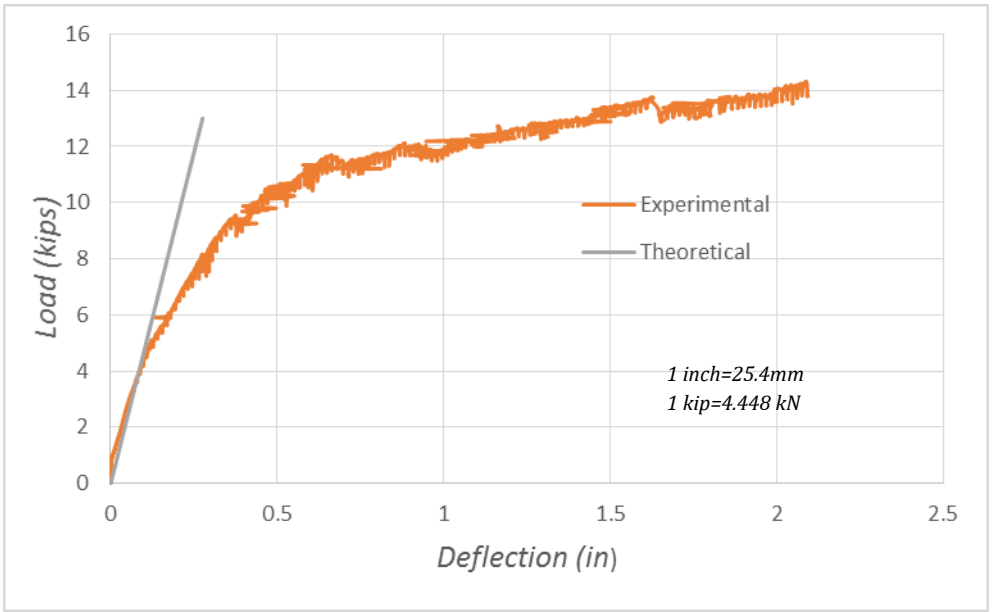

Figure (4.5): Comparison of Experimental and Theoretical Deflection for Slab Specimen "C"

By comparing the analytical and theoretical deflection curves we can see that analytical results can estimate the linear response with high level of accuracy. Also, the experimental results show that in reality after the slab specimens reach maximum linear deflection it follows non-linear behavior

For analytical calculations of slab specimen B and C, refer to Appendix A and Appendix B. Comparison of the experimental load capacity with predicted load capacity is summarized in Figure (4.6) and Table (4.1).

Figure(4.6): Comparison of Experimental Load Capacity with Predicted Load Capacity in Flexure.

In Figure (4.6), it is shown that the experimental load capacity for slab specimen A and B is higher than the predicted load capacity. This is due to two reasons. First, the assumptions made while calculating predicted load capacity are not always true. Second, the predicted

load capacity accounts only the linear behavior of slab specimens while experimental load capacity shows the non-linear behavior also of the slab specimens. Figure (4.6) also shows that the experimental load capacity of slab specimen C is less than the predicted load capacity. This is due to the reason that slab C was having larger span (172 in x172 in) as compared to the slab specimens A and B (132in x 132in) and therefore for predicted load capacity its rigidity was more and thus load capacity was more. But for this case, in reality, increase on rigidity does not affect experimental load capacity to a greater extent . Hence, experimental load capacity was not increased due to increase in rigidity. Table(4.1) shows the experimental and theoretical load values for all the three slab specimens.

Table (4.1): Comparison of Experimental and Theoretical loads

Sample	***Experimental Results, P (kips)***	***Analytical Flexural Capacity P (kips)***	***Analytical One-way Shear Capacity, P (kips)***	***Analytical Two-way Shear Capacity P (kips)***
Slab A	98.0(22.0)	76.0(17.0)	438.0(98.5)	141.0(31.7)
Slab B	89.0(20.0)	65.0(14.7)	438.0(98.5)	141.0(31.7)
Slab C	60.0(14.0)	83.0(18.65)	600.0(134.8)	141.0(31.7)

The toughness has been calculated as shown in Table (4.2) by integrating the area under load displacement curve for each of the three slab specimens**.**

Table (4.2): Toughness of the Slab Specimens

Slab Specimen	Toughness kNm(kip-ft)
A	248,366(37.0)
B	127,547(19.0)
C	164,468(24.5)

For all the three slabs the L/360 code serviceability deflection limit and the corresponding service load is summarized in Figures(4.7), (4.8), and (4.9).

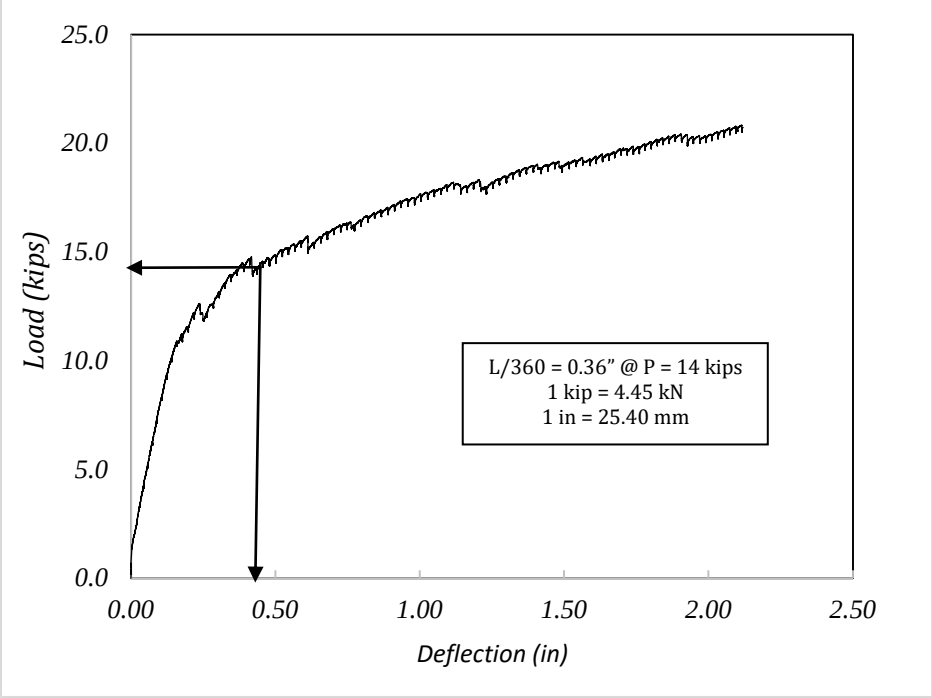

Figure (4.7): Determination of Service Load Capacity based on L/360 Deflection Limit Code Requirement for Sandwich Slab Specimen "A"

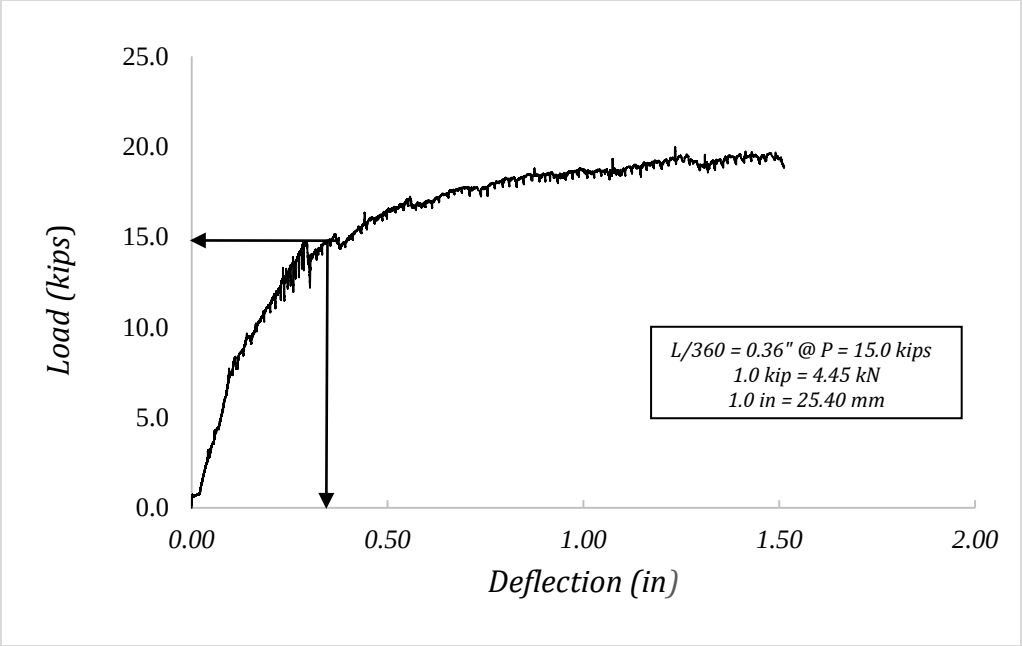

Figure (4.8): Determination of Service Load Capacity based on L/360 Deflection Limit Code Requirement for Sandwich Slab Specimen "B"

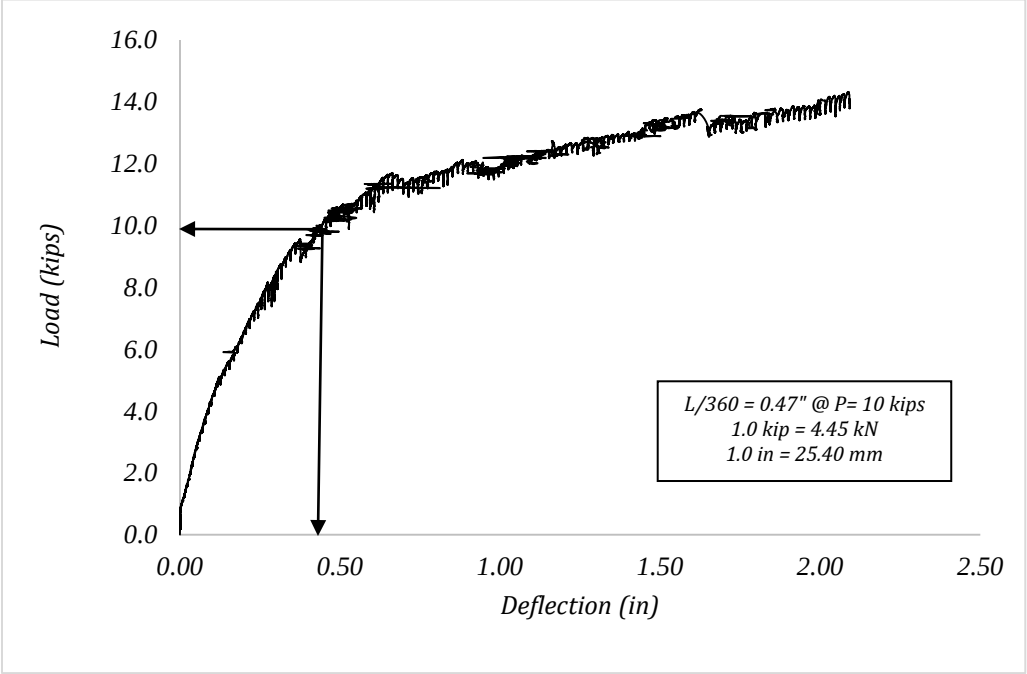

Figure (4.9): Determination of Service Load Capacity based on L/360 Deflection Limit Code Requirement for Sandwich Slab Specimen "C"

The comparison of service load capacity with the maximum experimental load capacity is summarized in Table (4.3)

Table(4.3): Comparison of Service and Experimental loads

Slab Specimen	**Service Load kN(kips)**	**Experimental Load kN(kips)**
A	62.27(14.0)	97.86(22.0)
B	66.72(15.0)	88.96(20.0)
C	44.48(10.0)	62.27(14.0)

The benefit of this is that these slab specimens can be used safely for residential buildings for maximum serviceable load (as mentioned in Table(4.3)) corresponding to serviceability deflection of L/360. But these slab specimens cannot be used for residential buildings subjected to loads higher than the service load capacity of the slab specimens (see Table(4.3))

CHAPTER 5

CONCLUSIONS AND RECOMMENDATIONS FOR FUTURE RESEARCH

5.1. General

This chapter presents a summary of the results and conclusions drawn from this research. In addition, recommendations for future research are also discussed and presented.

5.2. Conclusions

Based on the results obtained from the different sandwich slab specimen tests, the following conclusions are noted:

a) From the experimental results, it was found that slab specimen A had the highest flexural strength as compared to the other slab specimens evaluated in this study. As compared to slab specimen B with same span and slightly smaller thickness (12" vs 10.5"), the gain in the flexural strength was only 9%. This suggest that increasing the thickness has a minor effect on enhancing the flexural strength and that adding a supplemental hot–rolled steel reinforcement may have a larger impact in increasing both the strength and stiffness of such slabs. This issue can be confirmed by conducting additional tests in future.

b) In all the three slab specimens, based on the observed crack pattern, it is evident that the load is transferred in two directions and the slab specimens acted as two-way slab construction.

c) The ACI 318 analytical procedure was successful in predicting the strength of the

slabs, however; it was only successful in predicting the deflection at the linear range. This is expected due to local deformation of the parallel shear connectors and the possibility of losing the composite action of the sandwich slabs at higher loads. This fact was confirmed by the large difference between the predicted deflection at the ultimate load as compared to the large observed experimental deflection values (see Table (5.1)).

Table (5.1): Comparison of Predicted and Experimental Deflection.

Slab Specimen	**Predicted Deflection mm(inch)**	**Experimental Deflection mm(inch)**
A	4.57(0.18”)	56.38(2.22”)
B	5.33(0.21”)	38.10(1.50”)
C	11.18(0.44”)	53.34(2.10”)

d) Although the L/360 deflection code limit (see Table (4.3))was satisfied, however, these values were achieved at a higher load levels close to the ultimate load, leaving a minor space for a safety factor. This mandate that additional hot-rolled steel reinforcement be added in the tension side of these slabs to provide additional strength and stiffness and also to increase ductility of the sandwich slabs.

e) Related to the last point, it can be concluded that through-the-thickness parallel shear connectors play a major role in the resulting deflection especially in the non-linear range. For this reason, it is recommended to increase both the diameter and the

number of these connectors and pay much attention to the weld quality between the ends of these connectors with the exterior steel wire mesh.

5.3. Recommendations for Future Research

Based on the information learned during the course of this study, the following recommendations for future research are presented:

1- Additional study on studying the behavior of 3D sandwich slabs under different type of loading such as uniform distributed and four-point loading regimes are recommended.

2- Evaluation of the performance of these slabs when additional hot-rolled steel reinforcements are added will provide evidence on the potential stiffness and ductility enhancement of these slabs.

3- More studies are recommended to evaluate the behavior of such slabs when supported on different boundary conditions such as hinged and semi-rigid supports. In fact, the most reliable and practical supporting condition would be by using sandwich beams or sandwich wall panel supporting joints that mimic the actual building condition.

4- As described in this thesis, punching shear is considered to a critical design factor especially for sandwich structures with low shear transfer capacity. For this reason future studies on sandwich slabs subjected to punching shear are recommended.

5- The dynamic response of these types of panel system needs to be evaluated through both experimental and theoretical studies especially its capability to serve as lateral diaphragm for resisting lateral seismic forces in a typical building.

REFERENCES

- Acceptance Criteria AC 85(2014), Acceptance Criteria For Test Reports, International Code Council-Evaluation Service (ICC-ES), September, pp. 1-3.
- ACI318-14*Building Code Requirements for Structural Concrete (ACI 318-14)and Commentary,* American Concrete Institute, Farmington Hills, Michigan, USA.
- Bajracharya, R. M., 2010, *Structural Evaluation of Concrete-Expanded Polystyrene Sandwich Panels for Slab Applications*, Masters of Engineering Science thesis, University of Southern Queensland.
- Bangash, MYH 2001, Manual of numerical methods in concrete :modelling and applications validated by experimental and site-monitoring data, Thomas Telford,London.
- Chakrabarti, A & Sheikh, AH 2005, 'Analysis of Laminated Sandwich Plates Based on Interlaminar Shear Stress Continuous Plate Theory', *Journal of Engineering Mechanics*, vol. 131, no. 4, pp. 377-84.
- Davies, JM 1987, 'Axially Loaded Sandwich Panels', *Journal of Structural Engineering*, vol. 113, no. 11, pp. 2212-2230.
- Davies, JM (ed.) 2001, Lightweight Sandwich Construction, Blackwell Science, Oxford, UK.
- Eriksson, L. andR. Tränk, 1991. "*Properties of expanded polystyrene – Laboratory Experiments. Expanded Polystyrene as Light Fill Material*," Technical Visit around Stockholm - June 19, Internal Publication of the Swedish Geotechnical Institute, Linköping, Sweden.

- Horvath, J. S., 1994,"*Expanded Polystyrene (EPS) Geofoam: An Introduction to Material Behavior*," Geotextiles and Geomembranes, Vol. 13, pp. 263-280.
- Horvath, J.S., 1997,"*The Compressible Inclusion Function of EPS Geofoam*", *Geotextilesand Geomembranes*, vol. 15, nos. 1, 2, and 3, pp. 77-119.
- Magnan, J.-P. &Serratrice, J.-F. (1989). *"Propriétésmécaniques du polystyréneexpansé pour ses applications en remblairoutier,"* Bull. liaison Lab. Ponts. Chaussées, Vol. 164, pp. 25-31.
- Malhotra, V. M., 1999, "*Role of Supplementary cementing materials in reducing greenhouse gas emissions*," Proc. Int. Conference on Infrastructure Regeneration and Rehabilitation- Improving the Quality of Life through better Construction-A Vision for the Next Millennium, Ed. R.N. Swamy, Sheffield Academics Press, pp. 27-42.
- Manalo, AC 2011, "*Behaviour of fibre composite sandwich structures: a case study on railway sleeper application*", PhD thesis, University of Southern Queensland, Toowoomba, Australia.
- Mousa, MA &Uddin, N 2010, *"Experimental and Analytical Study of Composite Structural Insulated Floor Panels*", Honolulu, HI.
- Negussey, D. and M. Jahanandish, 1993, "*Comparison of Some Engineering Properties of Expanded Polystyrene with Those of Soils*", Transportation Research Record 1418, pp. 43-48.
- Pokharel, N., 2003, *"Behaviour and Design of Sandwich Panels Subject to Local Buckling and Flexural Wrinkling Effects*, PhD thesis, Queensland University of Technology,

Brisbane, Australia.

- Rizzo, S & Fazio, P 1983, *"Sandwich-Panel Assemblies: Analytical Model*,"*Journal ofStructural Engineering*, vol. 109, no. 11, pp. 2715-32.
- Schenker, A, Anteby, I, Nizri, E, Ostraich, B, Kivity, Y, Sadot, O, Haham, O, Michaelis, R, Gal, E & Ben-Dor, G 2005, *'Foam-Protected Reinforced Concrete Structures under Impact: Experimental and Numerical Studies'*, Journal of Structural Engineering, vol. 131, no. 8, pp. 1233-42.
- Sokolinsky, V.S., Shen, H, Vaikhanski, L & Nutt, SR 2003, *"Experimental and analytical study of nonlinear bending response of sandwich beams*", *Composite Structures*, vol. 60, no. 2, pp. 219-29.
- Ueng, CES 2001, Sandwich Composites, in AM Robert (ed.), *Encyclopedia of Physical Science and Technology*, Academic Press, New York, pp. 407-12.
- Vaidya, A, Uddin, N &Vaidya, U 2010, "*Structural Characterization of Composite structural Insulated Panels for Exterior Wall Applications*", *Journal of Composites for Construction*, vol. 14, no. 4, pp. 464-469.
- Warner, RF 2007, "*Reinforced concrete basics : analysis and design of reinforcedconcrete structures*," Pearson Prentice Hall, Frenchs Forest, N.S.W.
- Zenkert, D 1995, AnIntroduction to Sandwich Construction, Engineering Materials Advisory Services, Cradley Heath, West Midlands, England.

APPENDIX A

THEORETICAL LOAD CAPACITY FOR SLAB SPECIMEN B

A.1 Analytical calculation of Slab B

A.1.1 Flexure Analysis

Concrete strength: f'_c =33,750 kN/m^2(4895 psi), $\beta_1 = \frac{0.05(f'_c - 4000)}{1000} = 0.8$ (ACI 318-14 Table 22.2.2.4.3b)

Yield strength of steel: f_y= 3,86,106kN/mm^2 (56000 psi) at ε_{sy} = 0.00206

Clear span = slab width – 2* plate support at each side =132 - 2x9.5 =2.87m(113 in)

No. of steel wires along the width in the direction where the wires spacing is 3.15 = 113/3.15 = 36 wire

Diameter of one steel bar, d_b = 3 mm (0.1180 ″)

A_s for one steel bar =7 mm^2 (0.011 in^2)

Total tension steel area, A_s = *255 mm^2 (*0.396 in^2)

Modulus of Elasticity for steel = E_s=20 x 10^{10} (2.9 x 10^9 psi)

Assume C = the thickness of the concrete layer under compression =51mm (2.0 in)

The depth of Whitney stress block is found as,

$a = \ \beta_1 c = 0.8\ x\ 2 = 41mm\ (1.6\ in)$

For 10.5'' thick slab, the effective depth for tension steel is, d_t = (10.5 – 1.5 – 0.118/2) = 227 mm(8.94 in)

The strain in steel can be found out by similar triangle method as shown below,

$$\frac{\varepsilon_s}{(d_t - c)} = \frac{\varepsilon_{cu}}{c}$$

$$\frac{\varepsilon_s}{(8.94 - 2.00)} = \frac{0.0030}{2.00}$$

$\varepsilon_s = 0.0104 > \varepsilon_y = 0.0021$

Hence, assumption that steel has yielded in tension is correct. The nominal moment capacity of the cross is given by,

$$M_n = \ A_s f_y (d_t - \frac{a}{2})$$

$M_n = \ 0.396\ x\ 56\ x\ (8.94 - \frac{1.6}{2})$

$M_n =$ 180.5 kip-in = 20kN-m (15.04 kip-ft)

But;

$$M_n = 0.5\ pl/4 - 0.5\ wl^2/8$$

Where;

P: is concentrated load applied in the center line of the slab, and as soon as the slab is rectangular then the distribution factor for transferring load in two direction is 0.5.

W: is the own weight of the slab which is acting (downward) in the opposite direction of the applied load (upward), and as soon as the slab is rectangular then the distribution factor for transferring load in two direction is 0.5.

$$w = specific\ weight\ of\ the\ slab * weidth * thickness = \frac{145}{12 * 12 * 12} * 113 * 3.5$$

$$= 592\frac{kg}{m}(33.19\frac{lb}{in})$$

$$15.04 * 12 * 1000 = \frac{0.5\ P_n * 113}{4} - 0.5 * 33.19 * \ (113)^2/8$$

$$P_n = 65.38kN\ (14.7\ Kips)$$

A.1.2 Shear Analysis

The nominal shear strength shall be calculated ignoring the shear connectors contribution and taking only the thickness of concrete layer in tension side.

$$v_n = 2\sqrt{f'_c}\ b\ t = 2\ \sqrt{4895} * 113 * 1.5 = 105\ kN\ (23.7\ Kips) \quad \textit{ACI-318 14 Eq. 22.5.5.1}$$

But;

$$v_u = 0.5\ p/2 - 0.5\ wl/2$$

Where;

P: is concentrated load applied in the center line of the slab, and as soon as the slab is rectangular then the distribution factor for transferring load in two direction is 0.5.

W: is the own weight of the slab which is acting (downward) in the opposite direction of the applied load (upward), and as soon as the slab is rectangular then the distribution factor for transferring load in two direction is 0.5.

$$w = specific\ weight\ of\ concrete * weidth * thickness = \frac{145}{12 * 12 * 12} * 113 * 3.5$$

$$= \frac{592Kg}{m} = 33.19\ lb/in$$

$$v_u = v_n = 23.7 * 1000 = 0.5\ p/2 - 0.5 * 33.19 * 113/2$$

$$P_n = 438\ kN\ (98.55\ Kips)$$

A.1.3 Two Way Shear Analysis

The slab will also be susceptible for two-way shear at the location of loading plate as there is a possibility that the loading plate itself may punch through small thickness of concrete before actually reaching the actual flexural load. Hence, it is important to estimate the punching shear capacity of the slab and compare it with failure load under flexure. Figure 32-3 shows critical section for punching for slab concrete layer. As the weak polystyrene core is embedded in between concrete layers, the loading plate is likely to punch through the concrete layer in contact. Hence, considering 2" thick concrete slab, punching shear capacity for slab is estimated per ACI 318-14 as shown below,

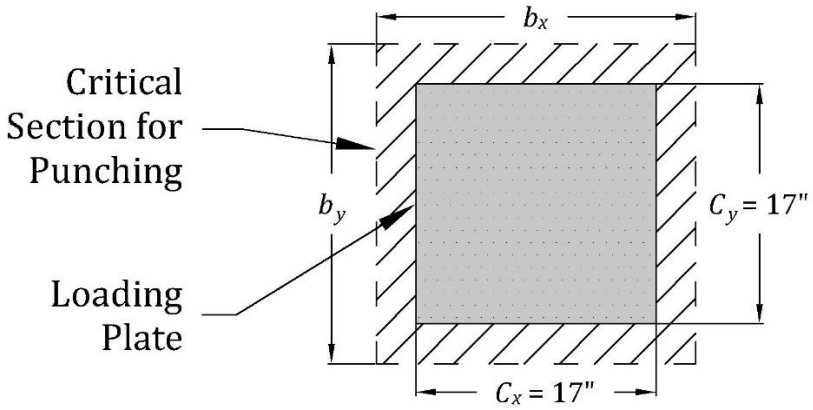

Figure (A.1): Critical Perimeter for Punching

Slab effective depth (d_{eff}) = compression side concrete - half of bar diameter =49mm (1.9410'')

$b_x = C_x + d_{eff}$= 18.941'' and $b_y = C_y + d_{eff}$ = 481mm (18.94'')

b_o = 2 x (b_x+ b_y) =1924mm (75.76'')

$A_c = b_o$ x d_{eff} = 94838mm^2 (147.0579 in^2)

α_s = 40 (assuming interior column condition)

$\beta_o = b_o / d$ = 37 and β_c = 1

ϕ = strength reduction factor = 0.75

Shear factor is considered minimum of the following:

S-Factor$_o$ = 2 + (α_s / β_o) = 3.08

S-Factor$_c$= 2 + (4 / β_c) = 6

S-Factor$_{max}$ = 4

S-Factor$_{controlled}$ = 3.08

v_n= S-Factor$_{controlled}$ ($\sqrt{f_c'}$) = 1486 kN/m^2 (215.5 psi)

The ultimate punching shear strength is computed as,

V_u= v_nx A_c= 215.5 x 147.0579 = 141 kN (31.7 kips)

Hence, flexural load capacity is lesser than the shear load capacity and punching load capacity. From the experimental observations, it can be confirmed that slab specimens have flexural failure as dominant failure mode and not the shear failure neither punching failure.

A.1.4 Deflection calculation of slab B

Specific weight of concrete used w = 2323Kg /m^3 (145pcf)

Total thickness = 266.7 mm (10.5 in)

F' $_c$ = 33759 kN/m^2(4895 psi)

E = 33 w$^{1.5}\sqrt{f_c}$ = 277 x 10^{5}kN/m^2= (4.03 x 10^6 psi)

$$G = \frac{E}{2(1+\nu)} = 1.679x10^6$$

Clear Span L = 2870 mm (113 in)

Panel Width = 1219 mm (48 in)

Center of gravity from the bottom line of the cross section, y is given as:

$$y = \frac{I_{top} \times y_{top} + I_{bottom} \times y_{bottom}}{I_{top} + I_{bottom}}$$

y = 91.18 mm (3.59 in)

$$I_{gross} = I_{top} + I_{bottom} + A_{top}(6.16)^2 + A_{bottom}(2.59)^2$$

I_{gross} = 142 x 10^7 mm^4 (3419.17 in^4)

$$I_{eff} = (0.2)I_{gross}$$

I_{eff}= 28 x 10^7 mm^4(683.83 in^4)

The slab is rectangular so the distribution factor is 0.5,

Basic deflection at the center of the panel at one direction, assumed hinged at both ends, given by:

δ = Flexure deflection + Shear deflection

$$\delta = \frac{0.5PL^3}{48EI_{eff}} + \frac{0.5PL}{4GAK_V}$$

Where;

P= Total applied load

E = concrete young's modules

I_{eff} = 0.2 I_{gross}

G = shear modulus

A = cross section area

Kv = the modified shear correction factor (Bank and Bednarczyk 1988)

$$K_v = \frac{A_{web}}{A_{gross}}$$

@ 48 in width we have six shear connector wires of diameter 0.118 in and with height of 7 in.

$$K_v = \frac{A_{web}}{A_{gross}} = \frac{(6)(0.118)(7)}{(6)(0.118)(7) + (48)(3.5)} = 0.029$$

$$\delta_{one\ direction} = \frac{(0.5)(P)L^3}{(48)(E)I_{eff}} + \frac{(0.5)(P)L^3}{(4)k_w(G)}$$

The total deflection at the center can be computed by the summation of the deflection in both sides, but the slab is rectangular then total deflection will be twice the deflection in one direction

$$\delta_{Total} = 2\left[\frac{(0.5)(P)L^3}{(48)(E)I_{eff}} + \frac{(0.5)(P)(L)}{(4)K_v(G)(A)}\right]$$

$$\delta_{Total} = 10.90 \times 10^{-3}P + 3.646 \times 10^{-3}P \qquad \text{Equation (1)}$$

Where P is in (kips) and δ is in (inch)

APPENDIX B

THEORETICAL LOAD CAPACITY FOR SLAB SPECIMEN C

B.1. Flexure Analysis

Concrete strength: f'_c =33750 kN/m^2(4895psi) , $\beta_1 = \frac{0.05(f'_c - 4000)}{1000} = 0.8$ (ACI 318-14 Table 22.2.2.4.3b)

Yield strength of steel: f_y= 3,86,106kN/mm^2 (56000 psi) at ε_{sy} = 0.00206

Clear span = slab width – 2* plate support at each side =172 - 2x9.5 = 3886 mm (153 in)

No. of steel wires along the width in the direction where the wires spacing is 3.15 = 153/3.15 = 49 wire

Diameter of one steel bar, d_b= 3 mm (0.1180 ″)

A_s for one steel bar =7.09 mm^2(0.011 in^2)

Total tension steel area, A_s = 255 mm^2(0.539 in^2)

Modulus of Elasticity for steel = E_s= 20 x 10^{10}kN/m^2 (2.9 x 10^9 psi)

Assume C = the thickness of the concrete layer under compression = 51 mm (2.0 in)

The depth of Whitney stress block is found as,

$a = \beta_1 c = 0.8\ x\ 2 = 41mm\ (1.6\ in)$

For 12'' thick slab, the effective depth for tension steel is, d_t = (12 – 1.5 – 0.118/2) = 265 mm (10.44 in)

The strain in steel can be found out by similar triangle method as shown below,

$$\frac{\varepsilon_s}{(d_t - c)} = \frac{\varepsilon_{cu}}{c} \qquad (i)$$

$$\frac{\varepsilon_s}{(10.4410 - 2.0000)} = \frac{0.0030}{2.0000}$$

$$\varepsilon_s = 0.0126 > \varepsilon_y = 0.0021$$

Hence, assumption that steel has yielded in tension is correct. The nominal moment capacity of the cross is given by,

$$M_n = A_s f_y \left(d_t - \frac{a}{2}\right) \qquad (ii)$$

$$M_n = 0.539\ x\ 56\ x\ (10.4410 - \frac{1.6}{2})$$

$M_n =$ 291 kip-in = 33kN-m (24.25 kip-ft)

But;

$$M_n = 0.5\ pl/4 - 0.5\ wl^2/8 \qquad (iii)$$

Where;

P: is concentrated load applied in the center line of the slab, and as soon as the slab is rectangular then the distribution factor for transferring load in two direction is 0.5.

W: is the own weight of the slab which is acting (downward) in the opposite direction of the applied load (upward), and as soon as the slab is rectangular then the distribution factor for transferring load in two direction is 0.5.

$$w = specific\ weight\ of\ the\ slab * weidth * thickness = \frac{145}{12 * 12 * 12} * 153 * 3.5$$

$$= 592\frac{kg}{m} = 44.93\ lb/in$$

$$24.25 * 12 * 1000 = \frac{0.5\ P_n * 153}{4} - 0.5 * 44.93 * \ (153)^2/8$$

$$P_n = 83kN\ (18.65\ Kips)$$

B.2 Shear Analysis

The nominal shear strength shall be calculated ignoring the shear connectors contribution and taking only the thickness of concrete layer in tension side.

$$v_n = 2\sqrt{f'_c}\ b\ t = 2\ \sqrt{4895} * 153 * 1.5 = 142\ kN\ (32\ Kips) \quad \textit{ACI-318 14 Eq. 22.5.5.1}$$

But;

$$v_u = 0.5\ p/2 - 0.5\ wl/2 \qquad (iv)$$

Where;

P: is concentrated load applied in the center line of the slab, and as soon as the slab is rectangular then the distribution factor for transferring load in two direction is 0.5.

W: is the own weight of the slab which is acting (downward) in the opposite direction of the applied load (upward), and as soon as the slab is rectangular then the distribution factor for transferring load in two direction is 0.5.

$$w = specific\ weight\ of\ concrete * weidth * thickness = \frac{145}{12 * 12 * 12} * 153 * 3.5$$

$$= 592\frac{kg}{m} = 44.93\ lb/in$$

$$v_u = v_n = 32 * 1000 = 0.5\frac{p}{2} - 0.5 * 44.93 * 153/2$$

$$P_n = 600kN\ (134.87\ Kips)$$

B.3. Two Way Shear Analysis

The slab will also be susceptible for two-way shear at the location of loading plate as there is a possibility that the loading plate itself may punch through small thickness of concrete before actually reaching the actual flexural load. Hence, it is important to estimate the punching shear capacity of the slab and compare it with failure load under flexure. Figure 32-3 shows critical section for punching for slab concrete layer. As the weak polystyrene core is embedded in between concrete layers, the loading plate is likely to punch through the concrete layer in contact. Hence, considering 2" thick concrete slab, punching shear capacity for slab is estimated per ACI 318-14 as shown below,

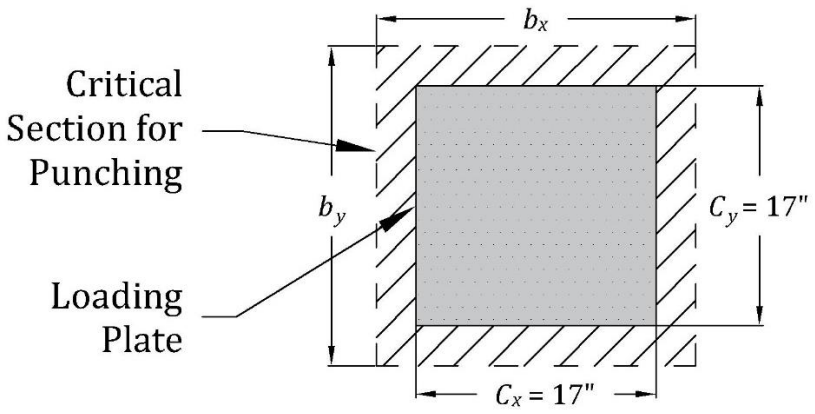

Figure (B.1): Critical Perimeter for Punching

Slab effective depth (d_{eff}) = compression side concrete - half of bar diameter = 1.9410''

$b_x = C_x + d_{eff}$ = 18.941'' and $b_y = C_y + d_{eff}$ = 481 mm (18.94'')

b_o = 2 x (b_x + b_y) = 1924 mm (75.76'')

$A_c = b_o$ x d_{eff} = 94838 mm^2 (147.0579 in^2)

α_s = 40 (assuming interior column condition)

$\beta_o = b_o / d$ = 37 and β_c = 1

ϕ = strength reduction factor = 0.75

Shear factor is considered minimum of the following:

S-Factor$_o$ = 2 + (α_s / β_o) = 3.08

S-Factor$_c$= 2 + (4 / β_c) = 6

S-Factor$_{max}$ = 4

S-Factor$_{controlled}$ = 3.08

v_n= S-Factor$_{controlled}$ ($\sqrt{f_c'}$) = 1486 kN/m^2 (215.5 psi)

The ultimate punching shear strength is computed as,

$V_u = v_n x A_c$= 215.5 x 147.0579 = 141 kN (31.7 kips)

Hence, flexural load capacity is lesser than the shear load capacity and punching load capacity. From the experimental observations, it can be confirmed that slab specimens have flexural failure as dominant failure mode and not the shear failure neither punching failure.

B.4. Deflection Calculation of Slab C

Specific weight of concrete used w =2323kg/m^3 (145 pcf)

F'$_c$ =33750 kN/m^2 (4895 psi)

E = 33 w$^{1.5}\sqrt{f_c}$ =277 X 10^{5}kN/m^2 (4.03 x 10^6 psi)

$$G = \frac{E}{2(1+\nu)} = 1.679x10^6$$

Clear Span L = 3886 mm(153 in)

Panel Width = 1219 mm (48 in)

Center of gravity from the bottom line of the cross section, y is given as:

$$y = \frac{I_{top} \times y_{top} + I_{bottom} \times y_{bottom}}{I_{top} + I_{bottom}}$$

y = 103 mm (4.04 in)

$I_{gross} = I_{top} + I_{bottom} + A_{top}7.21^2 + A_{bottom}3.04^2$

I_{gross} = 194 x 10^7 mm^4 (4674 in^4)

$I_{eff} = (0.2)I_{gross}$

I_{eff}= 38 x 10^7 mm^4 (935 in^4)

The slab is rectangular so the distribution factor is 0.5,

Basic deflection at the center of the panel at one direction, assumed hinged at both ends, given by:

δ = Flexure deflection + Shear deflection

$$\delta = \frac{0.5PL^3}{48EI_{eff}} + \frac{0.5PL}{4GAK_V}$$

Where;

P= Total applied load

E = concrete young's modules

I_{eff} = 0.2 I_{gross}

G = shear modulus

A = cross section area

Kv = the modified shear correction factor (Bank and Bednarczyk 1988)

$$K_v = \frac{A_{web}}{A_{gross}}$$

@ 48 in width we have six shear connector wires of diameter 0.118 in and with height of 8.5 in.

$$K_v = \frac{A_{web}}{A_{gross}} = \frac{(6)(0.118)(8.5)}{(6)(0.118)(8.5) + (48)(3.5)} = 0.034$$

$$\delta_{one\ direction} = \frac{(0.5)(P)L^3}{(48)(E)I_{eff}} + \frac{(0.5)(P)L^3}{(4)k_w(G)}$$

The total deflection at the center can be computed by the summation of the deflection in both sides, but the slab is rectangular then total deflection will be twice the deflection in one direction

$$\delta_{Total} = 2\left[\frac{(0.5)(P)L^3}{(48)(E)I_{eff}} + \frac{(0.5)(P)(L)}{(4)K_v(G)(A)}\right]$$

$$\delta_{Total} = 19.7 \times 10^{-3}P + 4.15 \times 10^{-3}P \qquad \text{Equation (1)}$$

Where P is in (kips) and δ is in (inch)

APPENDIX C

PROPERTIES OF STRING POTENTIOMETER

The string potentiometers were used with the specifications as described as follows:

Parameter	**Value**
Linearity 10", 15", 20" & 25" Ranges	±0.15% Full Scale
Repeatability	±0.015% full scale
Resolution	Essentially Infinite
Construction	Aluminum Cover & Baseplate
Sensing Device	Precision Potentiometer
Connector	MS3102A-14S-6P
Wire Rope	Ø.016 Stainless Steel
Weight Up to 50”	1.0 lb. (0.45 Kg)
Input Impedance	1000Ω ±10%
Output Impedance	0-1000Ω
Excitation Voltage	30 Volts Max. AC or DC
Output Voltage Change Over Full Range of Transducer	92% to 98% of Excitation Voltage
Thermal Coefficient of Sensing Element	±100 PPM/o C max.

Operating temperature	-40o C to +95o C
Operating humidity	95%
R.H. max. non-condensing Vibration	15 G's 0.1 ms max.
Shock	50 G's 0.1 ms max.
Ingress Protection	NEMA 1, IP-40
Life for 10” to 50” ranges	500,000 full stroke cycle

Dimensional Information for the string potentiometers used is shown in Figure (C.1)

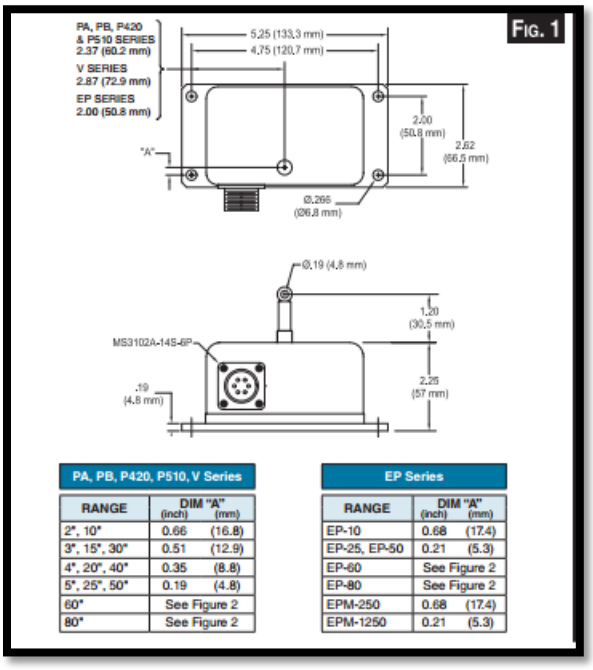

PA, PB, P420, P510, V Series		
RANGE	DIM "A" (inch)	(mm)
2", 10"	0.66	(16.8)
3", 15", 30"	0.51	(12.9)
4", 20", 40"	0.35	(8.8)
5", 25", 50"	0.19	(4.8)
60"	See Figure 2	
80"	See Figure 2	

EP Series		
RANGE	DIM "A" (inch)	(mm)
EP-10	0.68	(17.4)
EP-25, EP-50	0.21	(5.3)
EP-60	See Figure 2	
EP-80	See Figure 2	
EPM-250	0.68	(17.4)
EPM-1250	0.21	(5.3)

Figure (C.1): Dimensional Information for the String Potentiometer

APPENDIX D

MATLAB CODE USED TO ANALYSZE DATA

Matlab code used to plot P-delta curve for slab specimen A

```
A = SP1

B = SP2

C = SP3

D = SP4

A = A+1.13

For i= 1:80450

 If A(i, : ) < 0

A(i, : ) = 0;

Else

A(i, : ) = A(i, : );

End

End

E = sort (A)

F = Loadpsi

F = C*12.73

B = B+3.59

For i= 1:80450

 If B(i, : ) < 0
```

```
B(i, : ) = 0;
Else
B(i, : ) = B(i, : );
End
End
G = sort (B)
C = C +0.487
For i= 1:80450
 If C(i, : ) < 0
C(i, : ) = 0;
Else
C(i, : ) = C(i, : );
End
End
H = sort (C)
D = D+3.54
For i= 1:80450
 If D(i, : ) < 0
D(i, : ) = 0;
Else
D(i, : ) = D(i, : );
End
End
```

I = sort (D)

Plot(E,F,G,F,H,F,I,F)